NAS 1.14 D-8425

[illegible]

NASA TECHNICAL NOTE

NASA TN D-8425

NASA TN D-8425

COMPLETED
ORIGINAL

AILERON ROLL HYSTERESIS EFFECTS ON ENTRY OF SPACE SHUTTLE ORBITER

Richard W. Powell

Langley Research Center
Hampton, Va. 23665

NATIONAL AERONAUTICS AND SPACE ADMINISTRATION • WASHINGTON, D. C. • JULY 1977

(17)

1. Report No.	2. Government Accession No.	3. Recipient's Catalog No.
NASA TN D-8425		

4. Title and Subtitle	5. Report Date
AILERON ROLL HYSTERESIS EFFECTS ON ENTRY OF SPACE SHUTTLE ORBITER	July 1977
	6. Performing Organization Code

7. Author(s)	8. Performing Organization Report No.
Richard W. Powell	L-11010
	10. Work Unit No. 506-26-30-04
9. Performing Organization Name and Address NASA Langley Research Center Hampton, VA 23665	11. Contract or Grant No.
	13. Type of Report and Period Covered Technical Note
12. Sponsoring Agency Name and Address National Aeronautics and Space Administration Washington, DC 20546	14. Sponsoring Agency Code

15. Supplementary Notes

A portion of the material presented in this paper is contained in a thesis entitled "Effects of Control Hysteresis on the Space Shuttle Orbiter's Entry," submitted in partial fullfillment of the requirements for the degree of Master of Science, The George Washington University, June 1975.

16. Abstract

Six-degree-of-freedom simulations of the space shuttle orbiter entry with control hysteresis have been conducted on the NASA Langley Research Center interactive simulator known as the automatic reentry flight dynamics simulator. These simulations revealed that the vehicle can tolerate control hysteresis producing a ±50-percent change in the nominal aileron roll characteristics and an offset in the nominal characteristics equivalent to a ±5° aileron deflection with little increase in the reaction control system's fuel consumption.

17. Key Words (Suggested by Author(s))	18. Distribution Statement
Space shuttle orbiter Six-degree-of-freedom simulation Control hysteresis	Unclassified - Unlimited Subject Category 15

19. Security Classif. (of this report)	20. Security Classif. (of this page)	21. No. of Pages	22. Price*
Unclassified	Unclassified	47	$4.00

* For sale by the National Technical Information Service, Springfield, Virginia 22161

AILERON ROLL HYSTERESIS EFFECTS ON ENTRY OF SPACE SHUTTLE ORBITER*

Richard W. Powell
Langley Research Center

SUMMARY

Six-degree-of-freedom simulations of the space shuttle orbiter entry with aerodynamic control hysteresis were conducted on the NASA Langley Research Center interactive simulator known as the automatic reentry flight dynamics simulator. These simulations were performed to determine whether the presence of aerodynamic control hysteresis would affect the mission, either by making the vehicle unable to maintain proper attitude for a safe entry, or by significantly increasing the amount of required reaction control system fuel.

In the simulations, control hysteresis was modeled in the rolling moment due to aileron deflection. These simulations revealed that the vehicle can tolerate control hysteresis producing a $\pm$50-percent change in the nominal aileron characteristics and an offset in the nominal characteristics equivalent to a $\pm 5^{\circ}$ aileron deflection angle with little increase in the reaction control system's fuel consumption.

INTRODUCTION

A reusable Earth-to-orbit transportation system known as the space shuttle is being developed by the National Aeronautics and Space Administration (NASA). The space shuttle, consisting of an orbiter, an external fuel tank, and two solid rocket boosters will be capable of inserting payloads of 29 500 kg into a near-Earth orbit. The orbiter will be capable of retrieving payloads from orbit, entering, and landing with a payload of 14 500 kg. A general description of the orbiter configuration and mission is given in reference 1. In support of the shuttle program, the Langley Research Center has been studying the entry control characteristics of the space shuttle orbiter, with particular emphasis on the effects of aerodynamic phenomena on the vehicle during entry. One aerodynamic phenomenon which can occur is a variation of an aerodynamic force with control surface deflection which depends on the direction of travel of the surface. This phenomenon can appear as illustrated in sketch (a) and is referred to as control hysteresis. Wind-tunnel data from tests of early shuttle configurations indicated that control hysteresis could exist and could be a problem area during the entry of the space shuttle orbiters (ref. 2). It was shown that regions of shock-induced separated flow might be expected to exist on the leeward wing

*A portion of the material presented in this paper is contained in a thesis entitled "Effects of Control Hysteresis on the Space Shuttle Orbiter's Entry," submitted in partial fulfillment of the requirements for the degree of Master of Science, The George Washington University, June 1975.

Sketch (a)

surface and that upward deflected control surfaces could affect the extent of this separation. If the controls were deflected down into the wind, shock patterns from the surface might interact with the bow shock to cause unexpected separations. In addition, movement of a control surface into a vortex emanating from the wing leading edge, the wing fillet, or the vehicle nose might cause the vortex to burst. These phenomena may result in a lag in reestablishing flowfield equilibrium, and thus control hysteresis could exist.

Some unpublished results from wind-tunnel tests of a space shuttle orbiter model with remotely controlled elevons at $M = 10.3$ have indicated some evidence of aerodynamic hysteresis. The combination in these tests of a low reduced frequency parameter and low Reynolds numbers cast doubt on the validity of extrapolating the results to full-scale conditions. Because the wind-tunnel results were inconclusive, a six-degree-of-freedom simulation study was conducted to examine the impact of this potential problem. The simulation was conducted utilizing the automatic reentry flight dynamics simulator (ARFDS) (ref. 3) developed at the Langley Research Center.

Since the movement of the elevon surfaces occurs at a higher rate when these surfaces act as ailerons, hysteresis was modeled by offsetting and/or modifying the slope of the rolling moment due to aileron deflection so that the values of the rolling moment changed with the direction of control surface travel.

SYMBOLS

b wing span, m

c reference chord, m

C_l rolling-moment coefficient, $\dfrac{\text{Rolling moment}}{\bar{q}Sb}$

$C_{l_{\delta_a}} = \partial C_l / \partial \delta_a$

C_m pitching-moment coefficient, $\dfrac{\text{Pitching moment}}{\bar{q}Sc}$

C_1	control hysteresis coefficient
C_2	control hysteresis equivalent aileron deflection, deg
g	acceleration of gravity, m/sec^2
I_{sp}	specific impulse, sec
k_p	multiplier in $\delta_{a,c}$ block diagram
M	Mach number
p	roll rate about body axis, deg/sec
q	pitch rate about body axis, deg/sec
$\bar{q}$	free-stream dynamic pressure, Pa
r	yaw rate about body axis, deg/sec
r'	$= r - (180g \sin \phi \cos \theta)/Vw$, deg/sec
s	Laplacian operator
S	wing reference area, m^2
t	time, sec
V	velocity, m/sec
α	angle of attack, deg
α_c	commanded angle of attack sent to control system, deg
β	sideslip angle, deg
γ	flight-path angle, deg
δ_a	aileron deflection angle, deg
$\dot{\delta}_a$	$= d\delta_a/dt$, deg/sec
$\delta_{a,c}$	commanded aileron deflection angle, deg
$\delta_{a,UD}$	commanded aileron deflection angle required by up-down counter, deg
δ_e	elevator deflection angle, deg
δ_r	rudder deflection angle, deg
θ	pitch angle about body axis, deg

ϕ roll angle about body axis, deg

ϕ_c commanded roll angle, deg

Abbreviation:

RCS reaction control system

SPACE SHUTTLE ORBITER DESCRIPTION

The space shuttle orbiter (fig. 1) was designed to place and retrieve payloads in orbit, to perform an aerodynamic lifting entry from orbit, and to land on a prepared runway with a 14 500-kg payload. The aerodynamic performance capability of the orbiter is sufficient to provide an entry crossrange of 2040 km. In the normal operational mode, the orbiter entry is directed by onboard computers from deorbit through landing. A list of its physical parameters is shown in table I. The mission used in this study was a once-around return that had been launched into a 104° inclined orbit from the Western Test Range. Figure 2 depicts this entry on a world map, and figure 3 shows some of the trajectory parameters.

Guidance System

A closed-loop guidance system provides roll-angle and angle-of-attack commands for either the automatic flight control system or a pilot-operated, augmented flight control system. The entry guidance is designed to take the orbiter from 121.9 km, the atmospheric interface, down to 21.3 km, the beginning of the terminal area guidance phase. The roll-angle command controls downrange and crossrange, while the angle-of-attack command follows a preselected schedule. The guidance system is described in more detail in appendix A of reference 3.

Automatic Flight Control System

The control system, through the digital onboard computers, directs aerodynamic control-surface deflections and the reaction control system (RCS) jet firings. (See fig. 4.) The aerodynamic control surfaces include elevons, which are used as ailerons and elevators, a rudder with speed brake capability, and a body flap for longitudinal trim. RCS jets are also used for control about the roll, pitch, and yaw axes. The roll and pitch jets are used only during the early portion of the entry at low dynamic pressures. The jets have a nominal vacuum thrust of 3870 N. To approximate both the effects of thrust buildup with time and thrust loss due to increases in back pressure with decreasing altitude, a thrust level of 3336 N and an I_{sp} of 242 sec for each jet were used in this study.

The lateral directional portion of the control system operates in two basic modes. In the spacecraft mode ($\alpha > 18°$ or $M > 5$), ϕ_c from the guidance system is directed to the yaw RCS channel. This command produces a yawing rate and

a small β allowing the effective dihedral of the orbiter to generate a rolling moment. The ailerons are used for turn coordination. In the spacecraft mode, the rudder is not engaged. The control system switches to the aircraft mode when $\alpha \leq 15^{\circ}$ and $M \leq 5$. In this mode, the ailerons are used for ϕ control, and the rudder, now activated with yaw jet augmentation, is used for turn coordination. The speed brake and body flap deflections are based on a velocity schedule and a longitudinal center-of-gravity location, respectively. The control system is described in more detail in appendix B of reference 3.

AUTOMATIC REENTRY FLIGHT DYNAMICS SIMULATOR (ARFDS) DESCRIPTION

The control hysteresis effects were analyzed with the aid of the ARFDS. This is a nonlinear, six-degree-of-freedom, interactive, digital computer program developed by the Langley Research Center. This program utilizes hardware developed for real-time simulations. In addition, ARFDS includes an oblate rotating Earth model and uses nonlinear aerodynamics. ARFDS is operated from a control console where, at any time during the entry, control or guidance gains can be modified, winds or other disturbances can be added or removed, and guidance sampling frequency can be varied. However, no winds or gusts were considered in this study. The entry parameters can be observed on time-history strip charts; deficiencies can be noted; and appropriate solutions can be incorporated. ARFDS is described in more detail in reference 3.

WIND-TUNNEL RESULTS

Wind-tunnel tests were conducted in the Langley continuous-flow hypersonic tunnel using a space shuttle orbiter model with remotely controlled elevons (both left and right elevons move together). Data were taken at 40 samples/sec as the elevons were driven between their limits (-40° to 15° to -40°) at 6°/sec. Figure 5 shows representative pitching-moment (C_m) data fairings from these tests. The data fairings indicate that control hysteresis may be present. Although the control hysteresis observed in the data is very close to the balance accuracy, these trends repeated for all cases and thus indicated the possibility that control hysteresis did exist.

Test parameters, including a low reduced frequency parameter (model elevon rate scales to a full-scale rate of only 0.15°/sec, whereas the maximum full-scale rate is 20°/sec) and a low Reynolds number (1.0×10^6 based on length as compared with 5.0×10^6 full scale), made it impossible to predict the amount of full-scale control hysteresis that might be expected.

SIMULATION APPROACH

Since nominal entry simulation runs had indicated that the elevons are more active as ailerons than as elevons during the entry, an investigation was made with ARFDS where control hysteresis was added to the rolling moment (C_l) due to aileron deflection (δ_a).

If control hysteresis is present in the ailerons, two possible situations exist, depending on the flight conditions:

(1) In the spacecraft mode, the ailerons may be unable to coordinate the turn because as the ailerons deflect, the control system encounters off-nominal values of rolling moment. In addition, at these flight conditions, a lateral trim signal (see appendix B of ref. 3) is fed to the commanded aileron circuit to minimize RCS propellant consumption due to lateral center-of-gravity offsets and crosswind effects. This signal causes slight uncoordination of a roll maneuver; the ailerons then overshoot the proper position; and a reversal in the direction of the surface movement is required. Thus, the error signal in the commanded aileron circuit oscillates about zero. If this oscillation is larger than any built-in deadband, the ailerons also oscillate. Since the turn coordination signal is also fed to the roll thrusters while they are operational, and yaw-rate and roll-angle error signals are fed to the yaw thrusters, hysteresis in the aileron aerodynamic moments could result in alternate thruster firings and could sharply increase fuel consumption.

(2) In the aircraft mode, hysteresis could cause the orbiter to hunt continuously for the commanded roll angle, and since turn coordination is the responsibility of the rudder augmented by the yaw thrusters, this oscillation could produce alternate yaw thruster firings.

Thus, a major effect of control hysteresis was expected to be an increase in the amount of RCS fuel required for entry. Since the amount of fuel to be carried is limited, this increase could result in poor control of the orbiter and could limit its maneuverability.

Control hysteresis in C_l due to δ_a was modeled in two different forms as shown in figure 6. Figure 6(a) shows the first form where the nominal value of C_l is used for an increasing aileron deflection angle (δ_a positive) and the nominal value of C_l multiplied by C_1 is used for a decreasing deflection angle (δ_a negative). Multiplying C_l by C_1 changes the value of $C_{l_{\delta_a}}$. C_1 was varied from 0.5 to 1.5, and this variation provided a $\pm$50-percent change in the slope. For small values of δ_a, C_1 has little effect on C_l, as this method allows for no displacement of the origin. Thus, an increment C_2 (fig. 6(b)) was added to the nominal value if δ_a was negative. C_2 was expressed as an equivalent aileron deflection and was varied between $\pm 5^\circ$ of equivalent aileron deflection. Also C_1 and C_2 were applied simultaneously and resulted in the range of hysteresis shown in figure 6(c) for two representative Mach numbers, 4 and 10.

The aileron deflection remains zero until a dynamic pressure of 96 Pa is reached (nominally 320 sec after deorbit). The simulation on ARFDS was initiated at this point and continued until the terminal area guidance phase was encountered.

DISCUSSION OF RESULTS

The results of simulations for the nominal conditions ($C_1 = 1$; $C_2 = 0^\circ$) with a guidance system sampling time of 0.32 sec and a control system sampling time of 0.04 sec is shown on the time-history strip charts in figure 7. (See ref. 4 for further discussion on sampling rates.) As indicated previously, the ailerons are used for turn coordination until α is reduced to 18° (~1720 sec from deorbit). After that time, the ailerons are used for ϕ control, and the rudder assumes the coordination role. Times of increased aileron activity (namely between 400 and 500 sec from deorbit where ϕ increases from -15° to -75° and after 1500 sec where roll reversals occur) are times of increased RCS firings. Thus, adding hysteresis was expected to increase the RCS firings at these points and to result in more fuel consumption. Figures 8 and 9 show the effect of reducing C_1 to 0.7 and 0.5, respectively. Neither of these cases differs significantly from the nominal, either in the δ_a or the RCS thruster history. Returning C_1 to its nominal value of 1.0 and applying C_2 values of -2° (fig. 10) and -5° (fig. 11) produced similar results as did the combination of $C_1 = 0.5$ and $C_2 = -5^\circ$ (fig. 12). Table II shows the RCS fuel consumption for each of these cases in addition to cases for $C_1 = 1.5$ with $C_2 = 0^\circ$; $C_1 = 1$ with $C_2 = \pm 5^\circ$. These cases fall within 6 percent of the nominal.

During the time of the present study, separate studies indicated control system changes that permitted lower guidance sampling frequencies (2.00-sec sampling time) without limit cycling (ref. 4). The system changes were:

(1) Replacement of the step changes in commanded angle of attack and roll attitude with linear (ramp-like) changes.

(2) Modification of two gains in the control circuit.

Figures 13 to 18 show the results of applying control hysteresis to the simulation with the 2.00-sec guidance sampling time system, and again control hysteresis makes little difference in control surface and vehicle motion time histories. For these simulations, table III shows the fuel consumption caused by hysteresis.

It was noted that for most of the entry, $\delta_a = 0^\circ$ (figs. 7 to 18). It was therefore suspected that the aileron error signal remained within the deadband shown in the $\delta_{a,c}$ block diagram (fig. 19), and control hysteresis was thus prevented from having any significant effect. (Appendix B of ref. 3 includes an explanation of the operation of this filter.) Consequently, this deadband was removed from the circuit, and both a nominal ($C_1 = 1$; $C_2 = 0^\circ$) case and a control hysteresis case ($C_1 = 0.5$; $C_2 = 5^\circ$) were run with the nominal guidance scheme (0.32-sec sampling time). The aileron without the deadband becomes a continuously moving control in both cases just mentioned (figs. 20 and 21). Removal of the filter actually results in a reduction in fuel consumption from 176 kg to 156 kg for the no-hysteresis case. However, the addition of hysteresis results in significant increases in RCS fuel consumption (see table IV). Thus, the deadband filter in the aileron circuit acts to suppress the effects of any control hysteresis over the range of C_1 and C_2 tested.

In all cases when in the aircraft mode, aileron hysteresis had little effect on the entry (compare fig. 7 with figs. 8 to 12, fig. 13 with figs. 14 to 19, and fig. 20 with fig. 21). Thus, the hunt for the proper roll angle was sufficiently limited to insure that the rudder could provide turn coordination without additional aid from the yaw RCS.

CONCLUDING REMARKS

Using the automatic reentry flight dynamics simulator at the Langley Research Center, a six-degree-of-freedom simulation study was conducted on the entry of the space shuttle orbiter to determine whether control hysteresis in the rolling moment due to aileron deflection has any major effects on the controllability of the orbiter or whether hysteresis requires increased reaction control system fuel consumption. Control hysteresis was modeled by off-setting and/or modifying the slope of the roll due to aileron deflection so that the value of the rolling moment changed with the direction of control surface travel.

The simulations indicated that the orbiter system can tolerate control hysteresis producing a $\pm$50-percent change in the nominal characteristics and an equivalent $\pm 5^{\circ}$ aileron deflection with little increase in the required reaction control system's fuel consumption. This tolerance was traced to a deadband filter in the commanded aileron circuit. Removal of this filter resulted in significant increases in fuel consumption.

Langley Research Center
National Aeronautics and Space Administration
Hampton, VA 23665
April 14, 1977

REFERENCES

1. Malkin, M. S.: Space Shuttle/The New Baseline. Astronaut. & Aeronaut., vol. 12, no. 1, Jan. 1974, pp. 62-68.

2. Reding, J. Peter; and Ericsson, Lars E.: Review of Delta Wing Space Shuttle Vehicle Dynamics. Space Shuttle Aerothermodynamics Technology Conference, Vol. III - Aerodynamics, NASA TM X-2508, 1972, pp. 861-931.

3. Kaylor, Jack T.; Rowell, Lawrence F.; and Powell, Richard W.: A Real-Time Digital Computer Program for the Simulation of Automatic Spacecraft Reentries. NASA TM X-3496, 1977.

4. Powell, Richard W.; Stone, Howard W.; and Rowell, Lawrence F.: Effects of Modifications to the Space Shuttle Entry Guidance and Control Systems. NASA TN D-8273, 1976.

TABLE I.- PHYSICAL CHARACTERISTICS OF SPACE SHUTTLE ORBITER

Mass properties:	
Mass, kg	83 001
Moments of inertia:	
I_{XX}, kg-m^2	1 029 066
I_{YY}, kg-m^2	7 816 290
I_{ZZ}, kg-m^2	8 015 596
I_{XZ}, kg-m^2	177 612
I_{XY} and I_{YZ}	0
Wing:	
Reference area, m^2	249.91
Chord, m	12.06
Span, m	23.79
Elevon:	
Reference area, m^2	19.51
Chord, m	2.30
Rudder:	
Reference area, m^2	9.30
Chord, m	1.86
Body flap:	
Reference area, m^2	12.54
Chord, m	2.06

TABLE II.- REACTION CONTROL SYSTEM FUEL CONSUMPTION FOR NOMINAL SYSTEMS WITH GUIDANCE SAMPLING TIME OF 0.32 SECOND

C_1	C_2, deg	Fuel consumption, kg
1	0	176
.7	0	171
.5	0	195
1.5	0	174
1	-2	173
1	-5	181
1	+5	176
.5	-5	178

TABLE III.- REACTION CONTROL SYSTEM FUEL CONSUMPTION FOR REVISED SYSTEMS WITH GUIDANCE SAMPLING TIME OF 2.00 SECONDS

C_1	C_2, deg	Fuel consumption, kg
1	0	111
.7	0	112
.5	0	110
1	-2	111
1	-5	127
.5	-5	124

TABLE IV.- REACTION CONTROL SYSTEM FUEL CONSUMPTION FOR NOMINAL GUIDANCE WITH SAMPLING TIME OF 0.32 SECOND WITH AILERON DEADBAND FILTER REMOVED

C_1	C_2, deg	Fuel consumption, kg (a)
1	0	156
.5	-5	213

[a]Nominal entry (C_1 = 1; C_2 = 0°) with filter consumes 176 kg of reaction control system fuel.

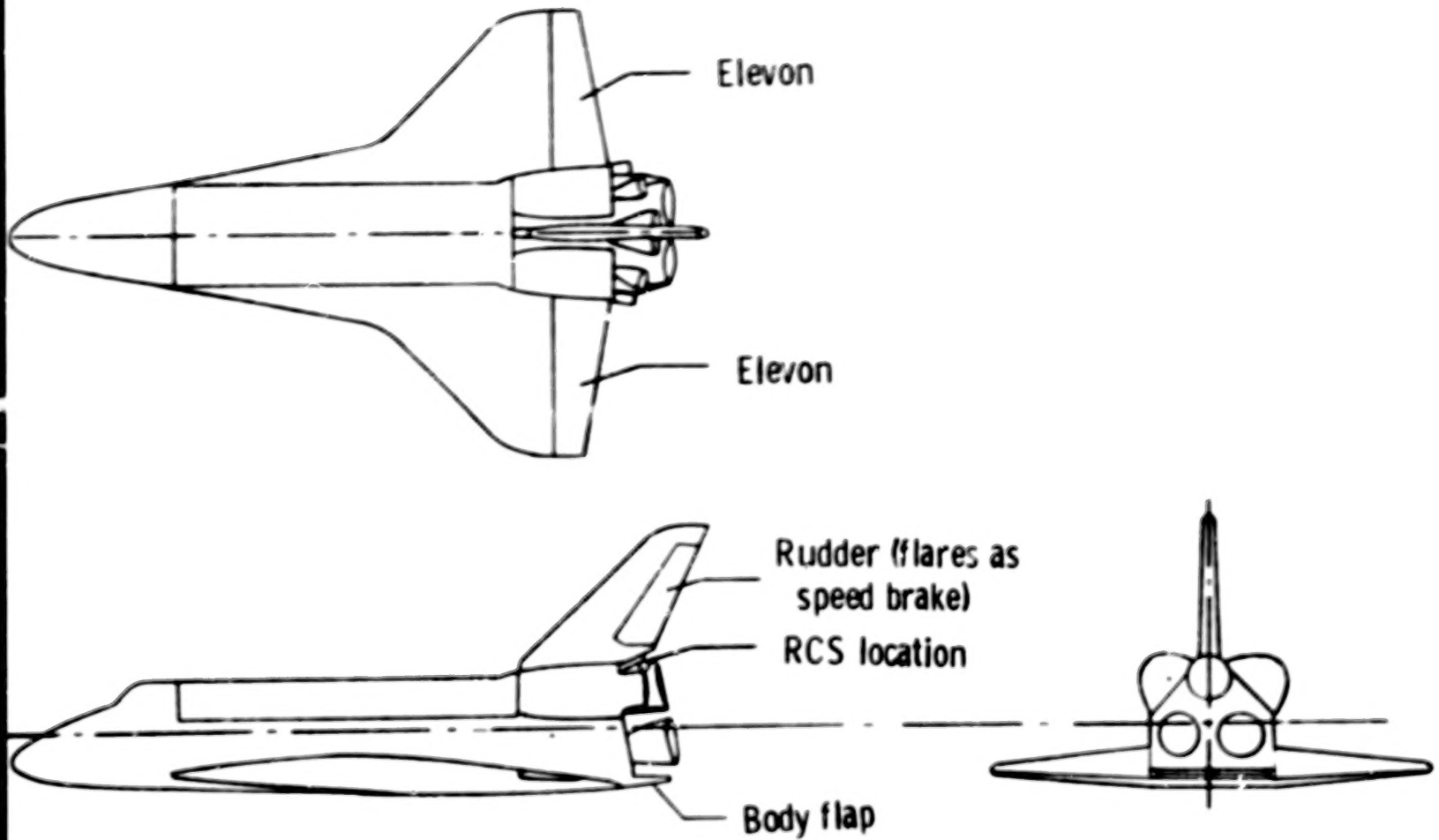

Figure 1.- Space shuttle orbiter.

Figure 2.- Space shuttle orbiter entry.

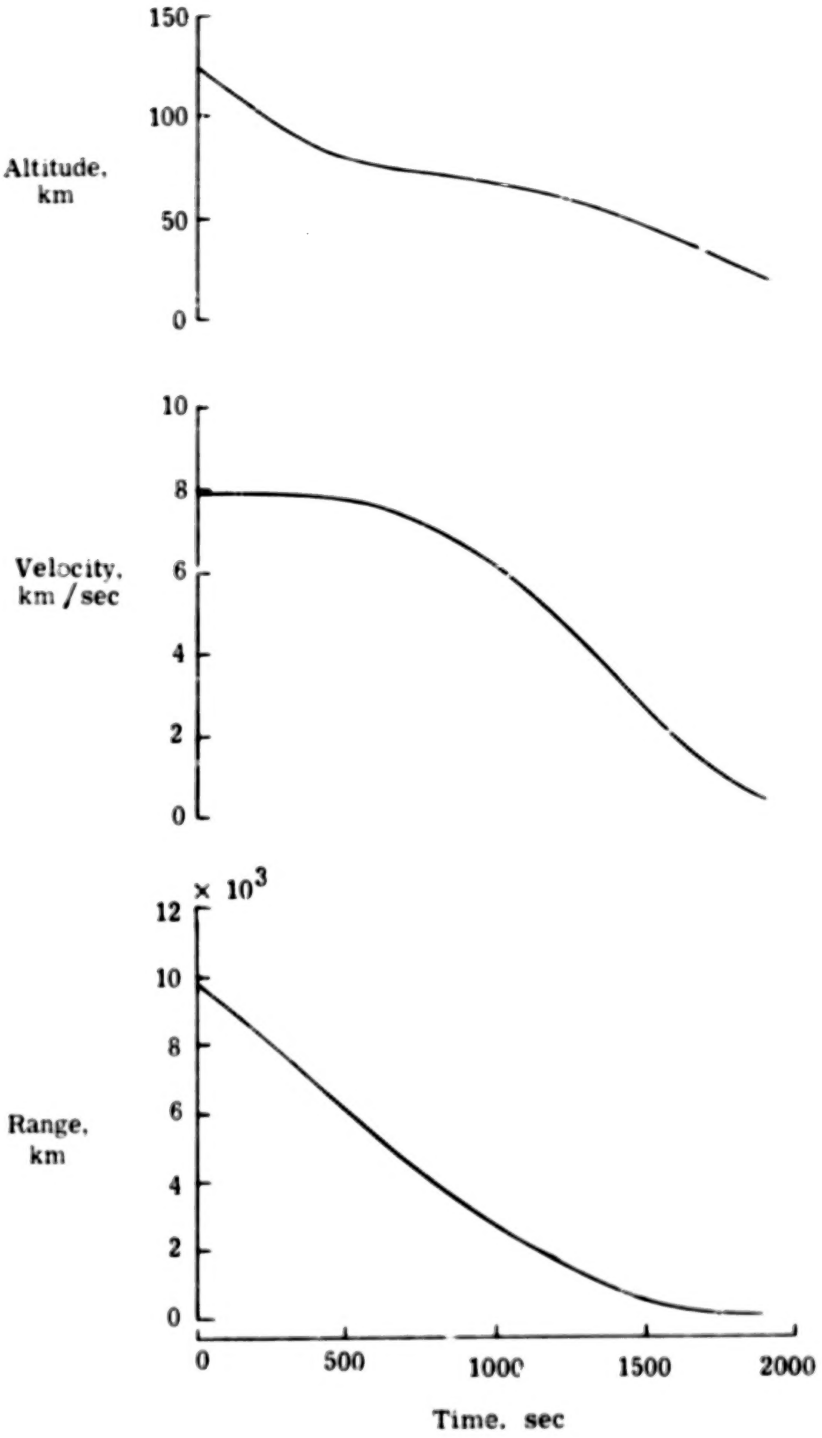

Figure 3.- Space shuttle orbiter entry trajectory parameters.

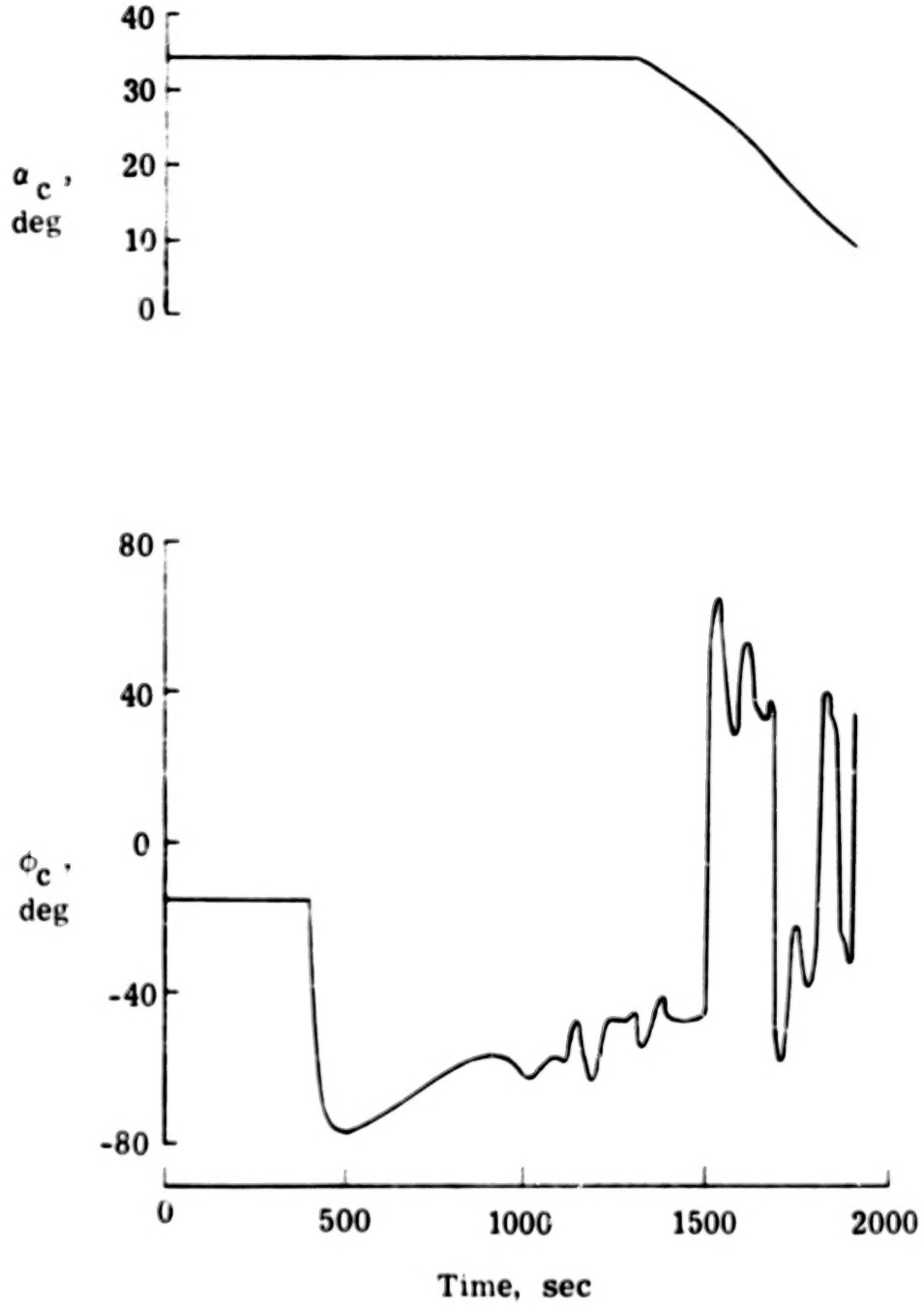

Figure 3.- Concluded.

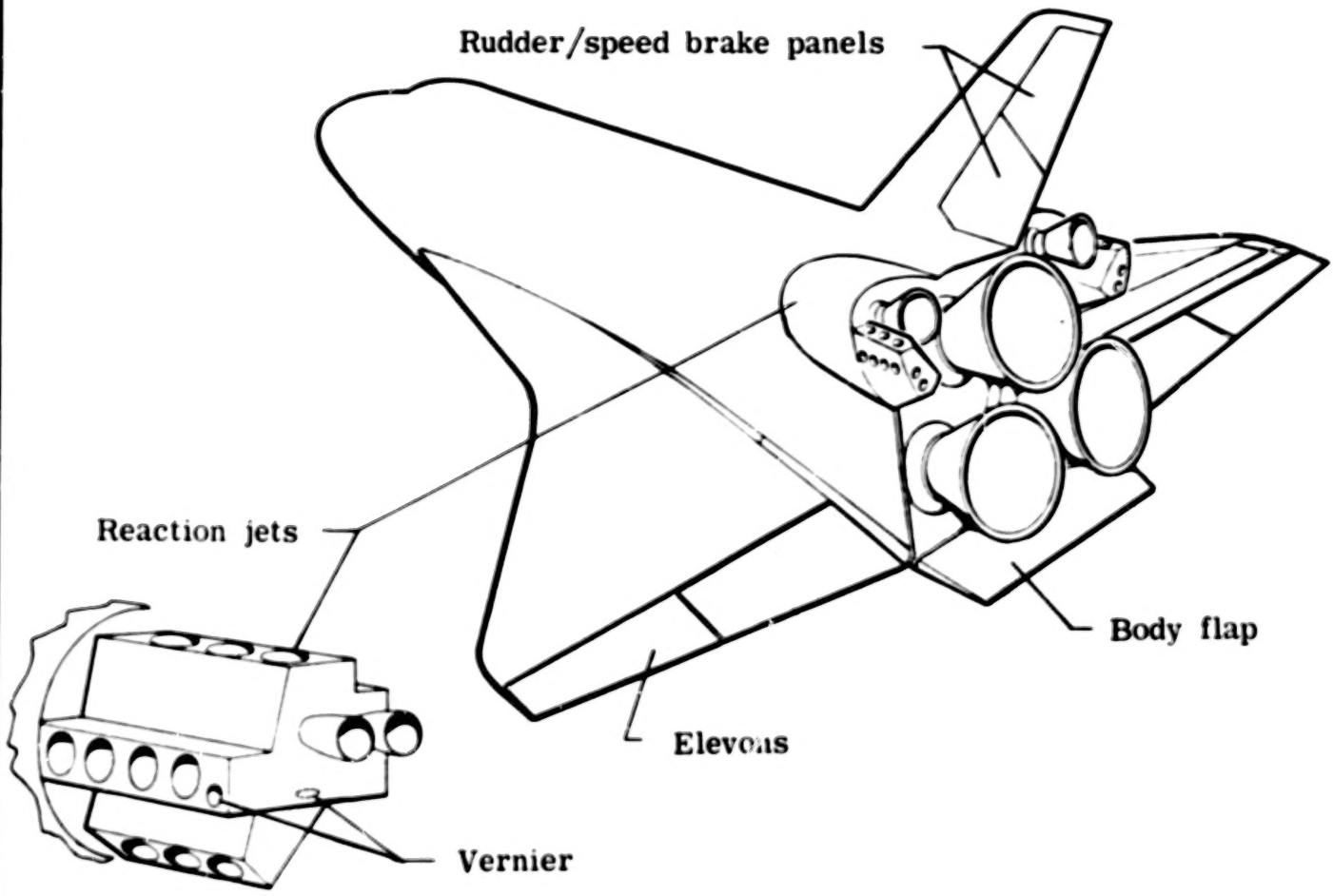

Figure 4.- Space shuttle orbiter; control system elements.

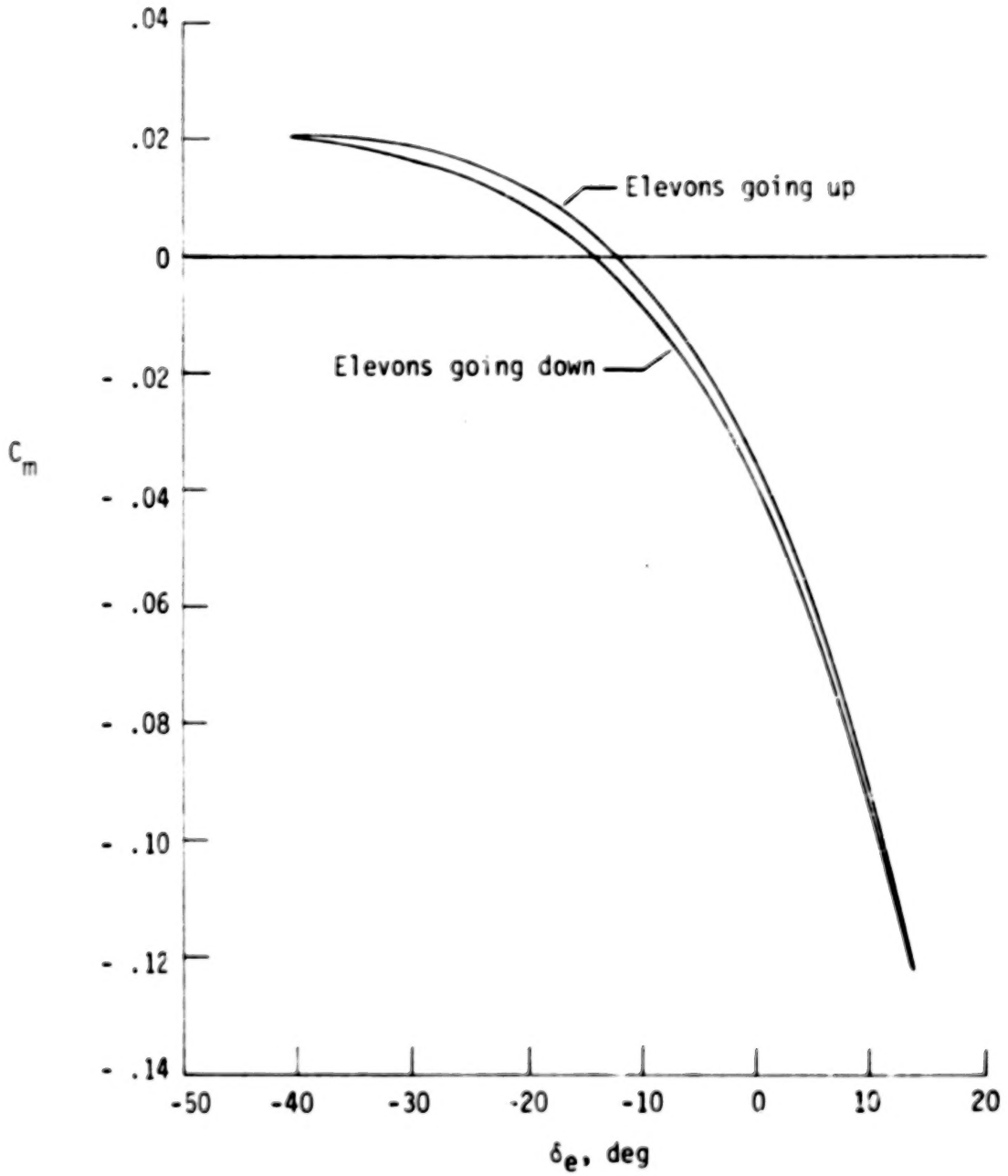

Figure 5.- Pitching-moment data for space shuttle orbiter model with remotely controlled elevons from Langley continuous-flow hypersonic tunnel.

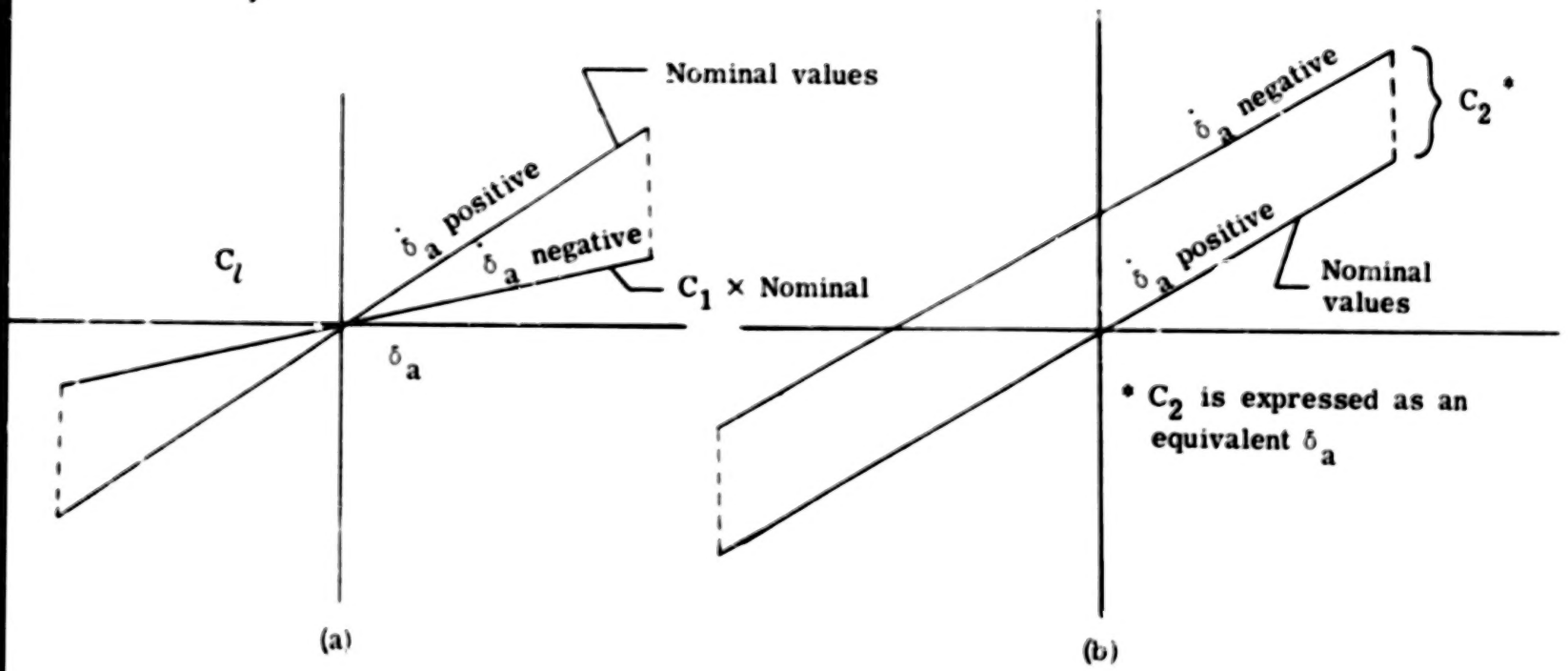

Figure 6.- Two hysteresis models.

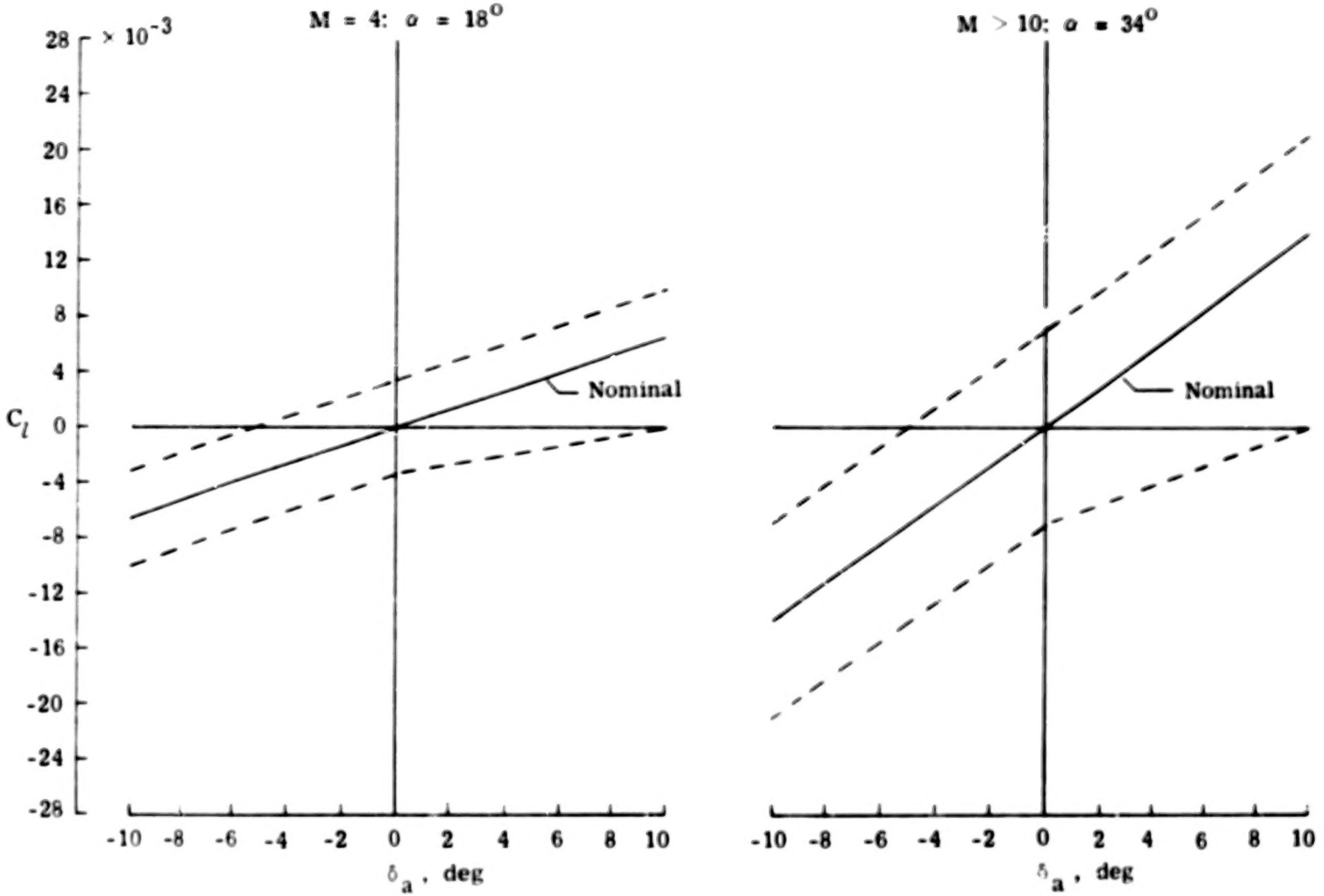

(c) Range of control hysteresis studied. Area between dashed lines indicates range of control hysteresis studied.

Figure 6.- Concluded.

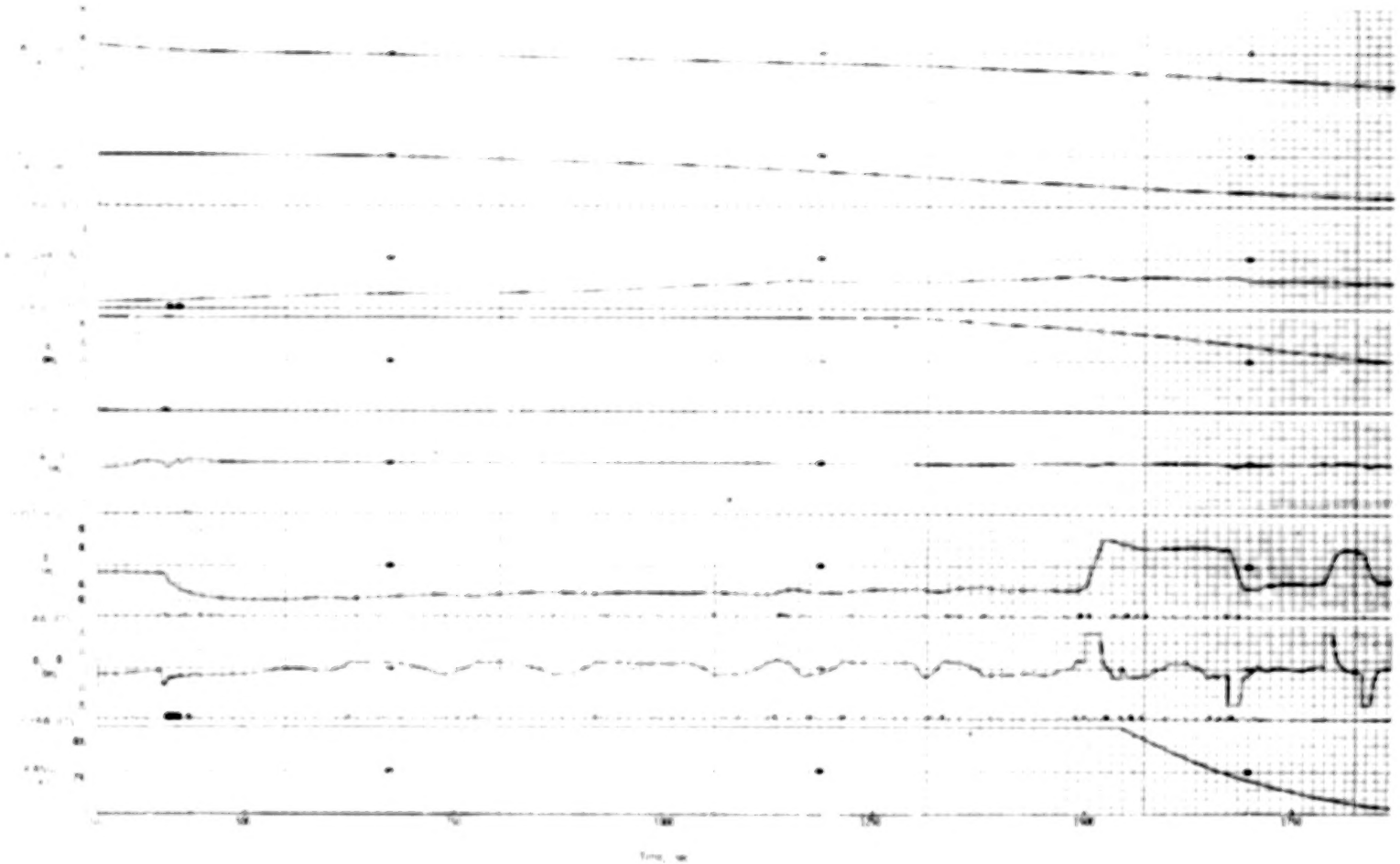

Figure 7.- Nominal guidance with no hysteresis.

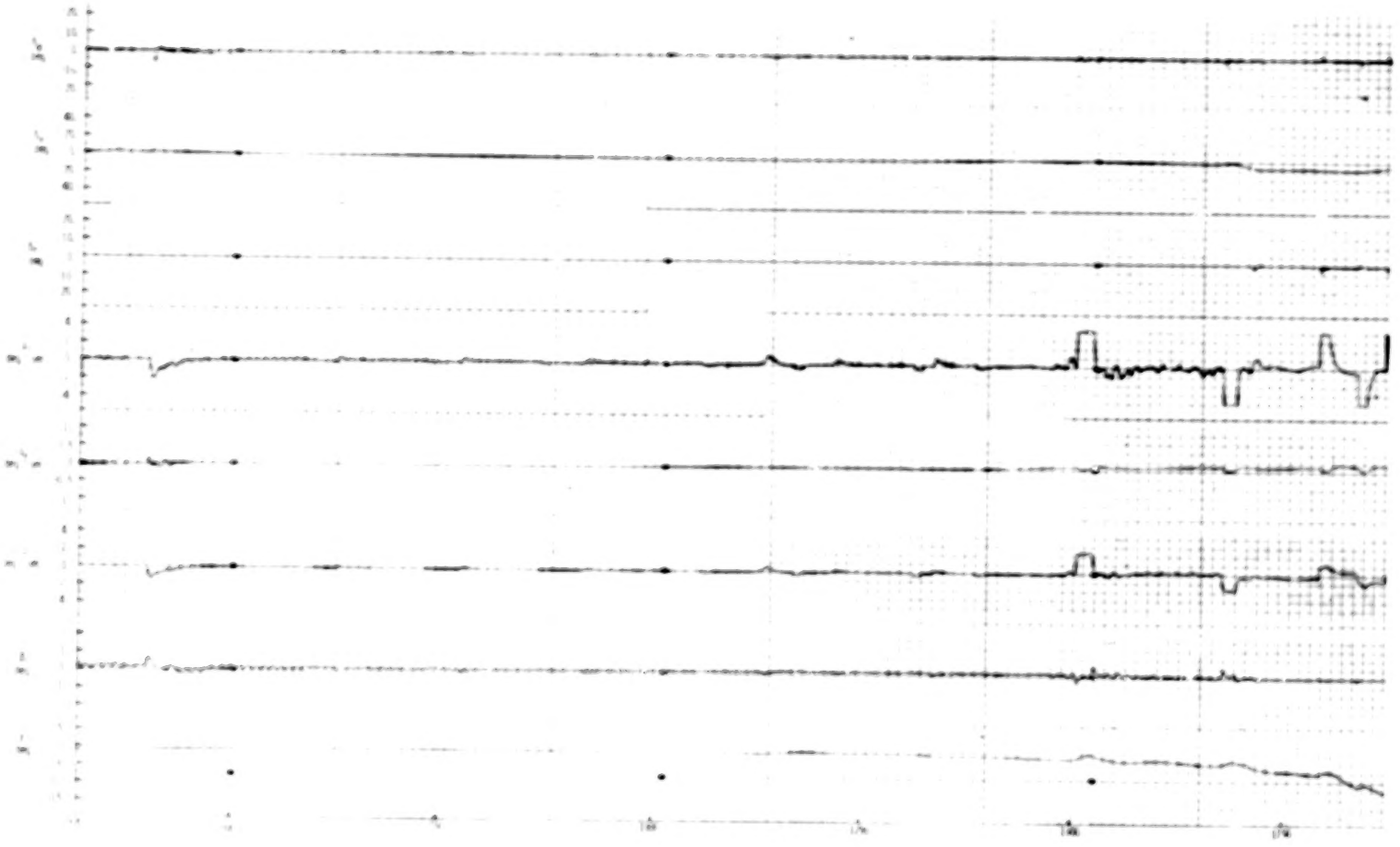

Figure 7.- Concluded.

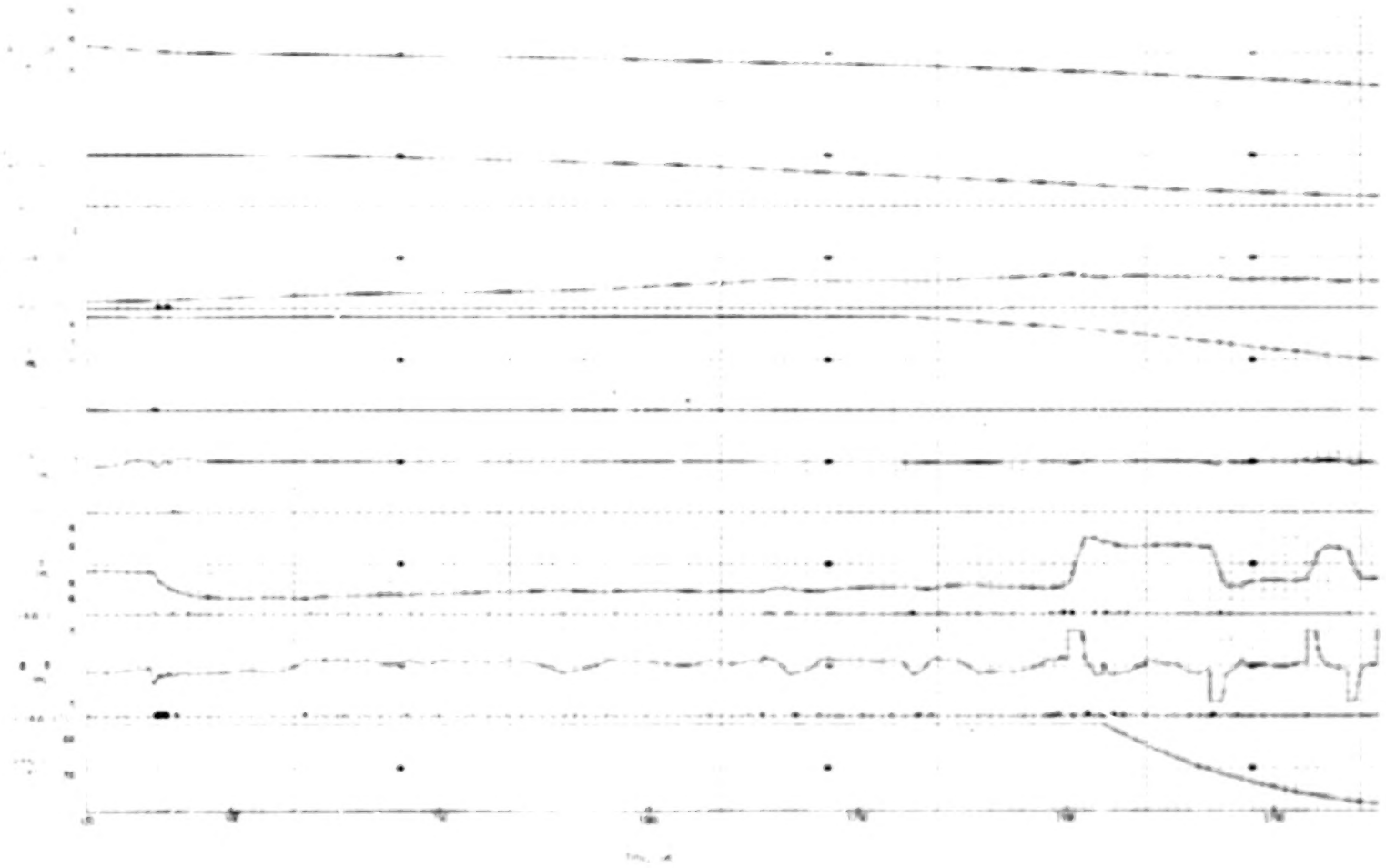

Figure 8.- Nominal guidance with hysteresis factors; $C_1 = 0.7$; $C_2 = 0^o$.

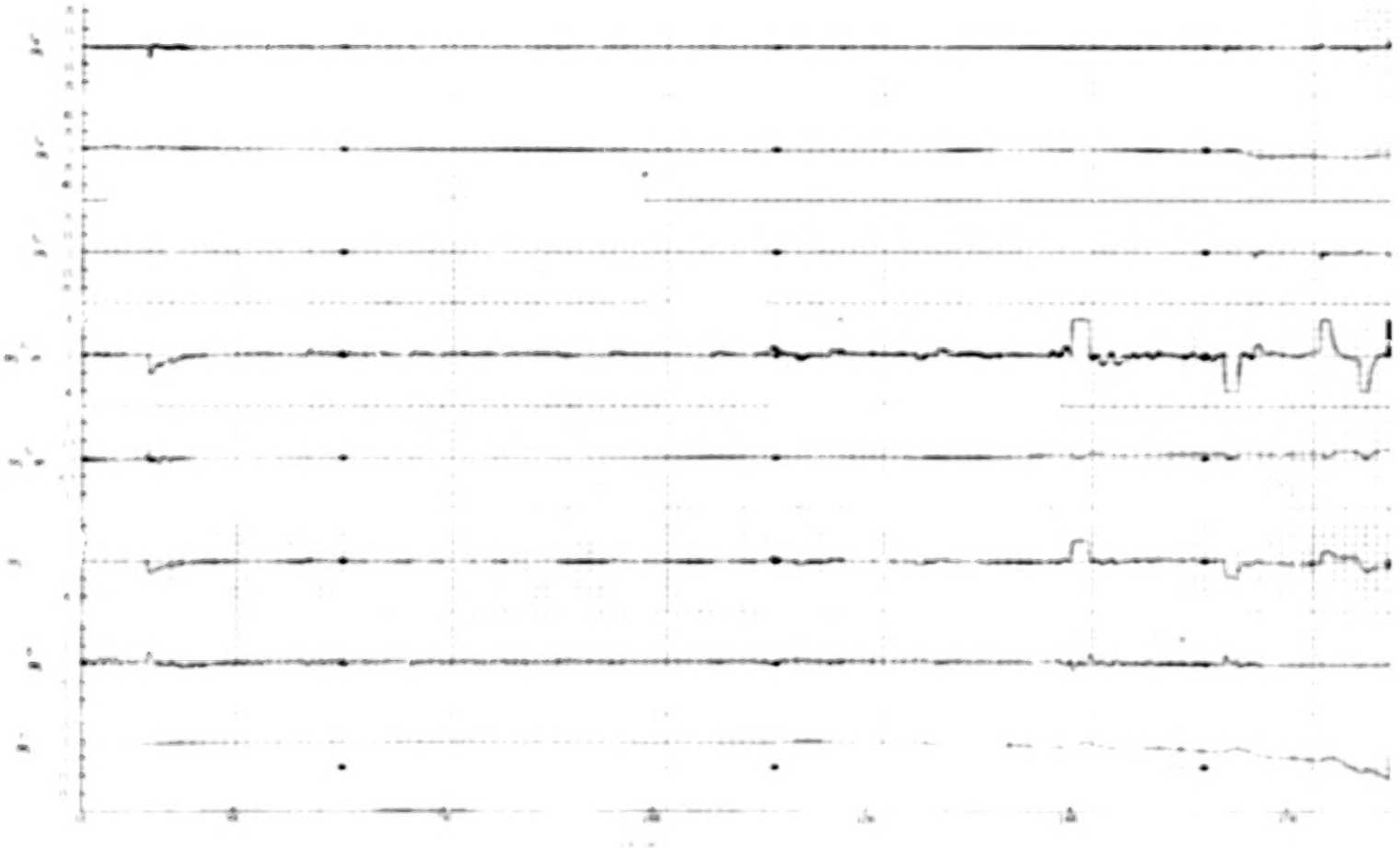

Figure 8.- Concluded.

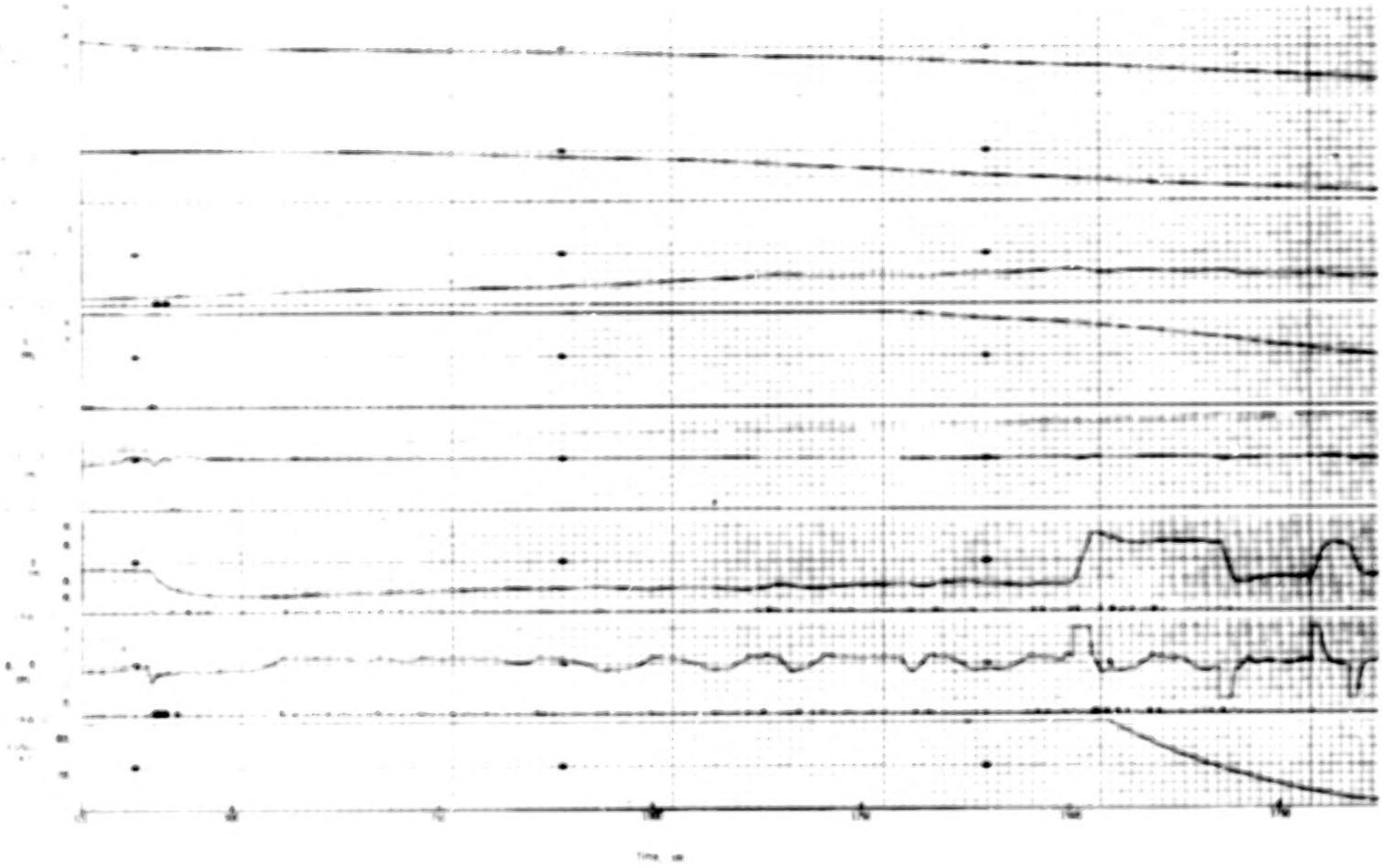

Figure 9.- Nominal guidance with hysteresis factors; $C_1 = 0.5$; $C_2 = 0^o$.

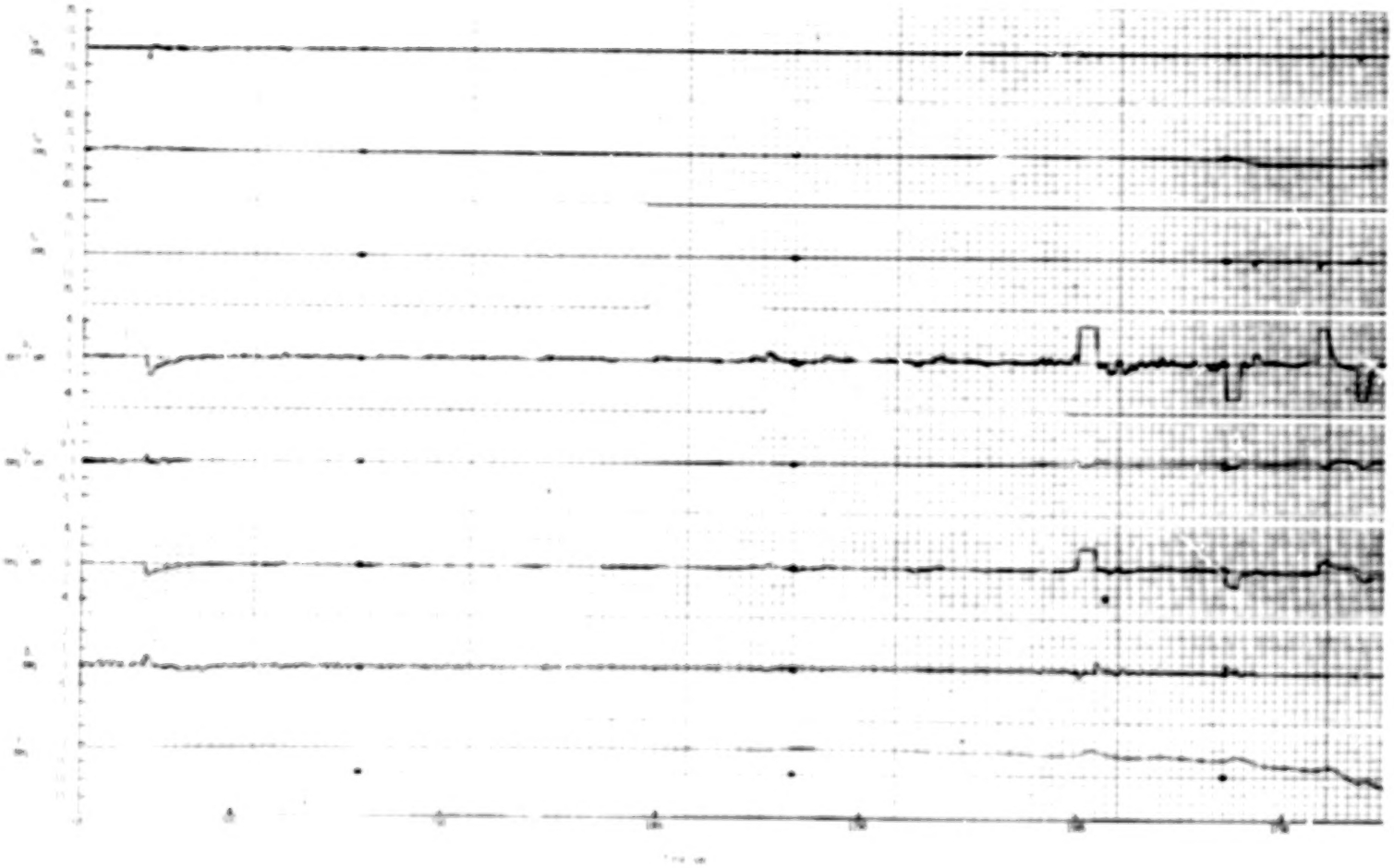

Figure 9.- Concluded.

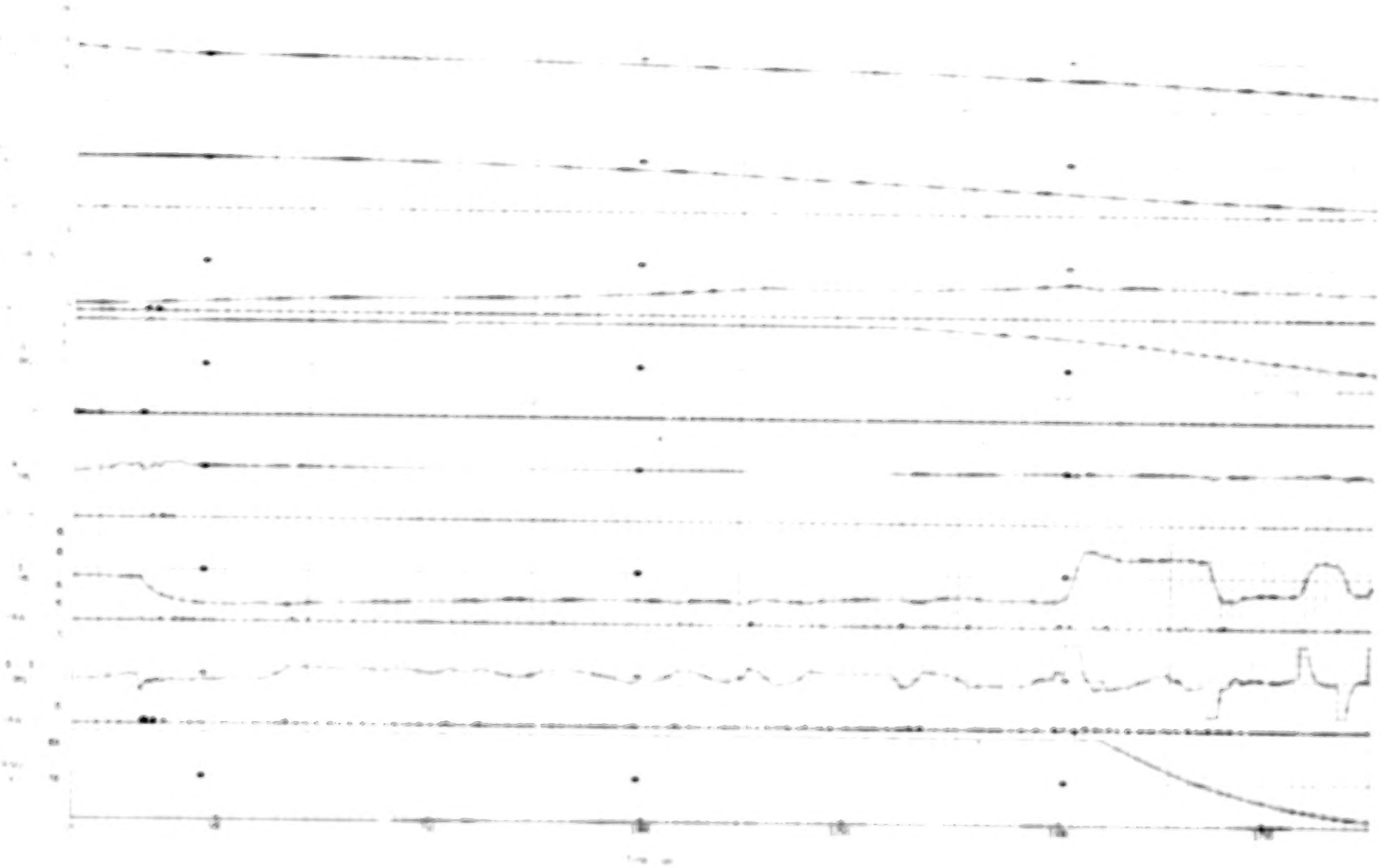

Figure 10.- Nominal guidance with hysteresis factors; $C_1 = 1.0$; $C_2 = 2^o$.

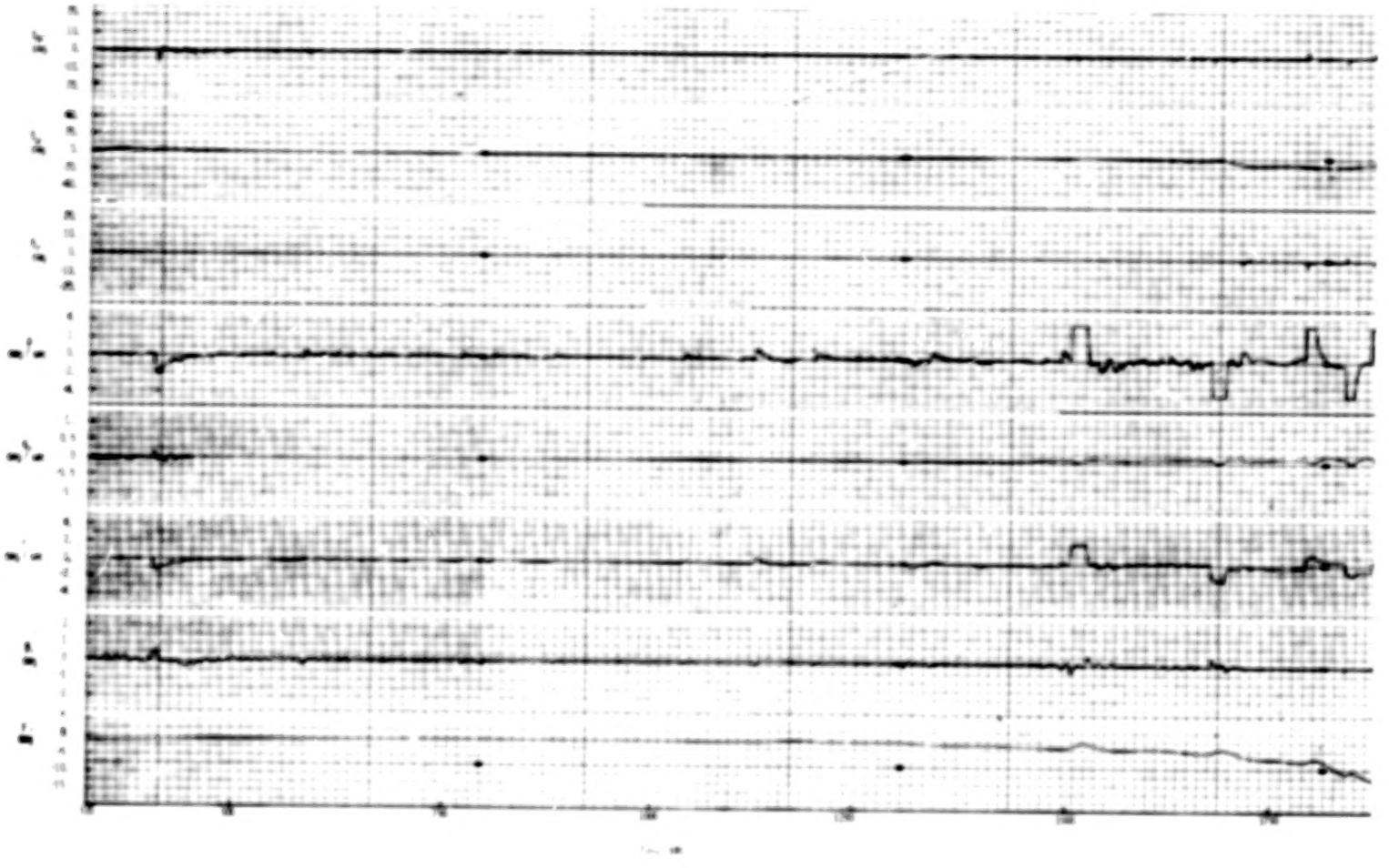

Figure 10.- Concluded.

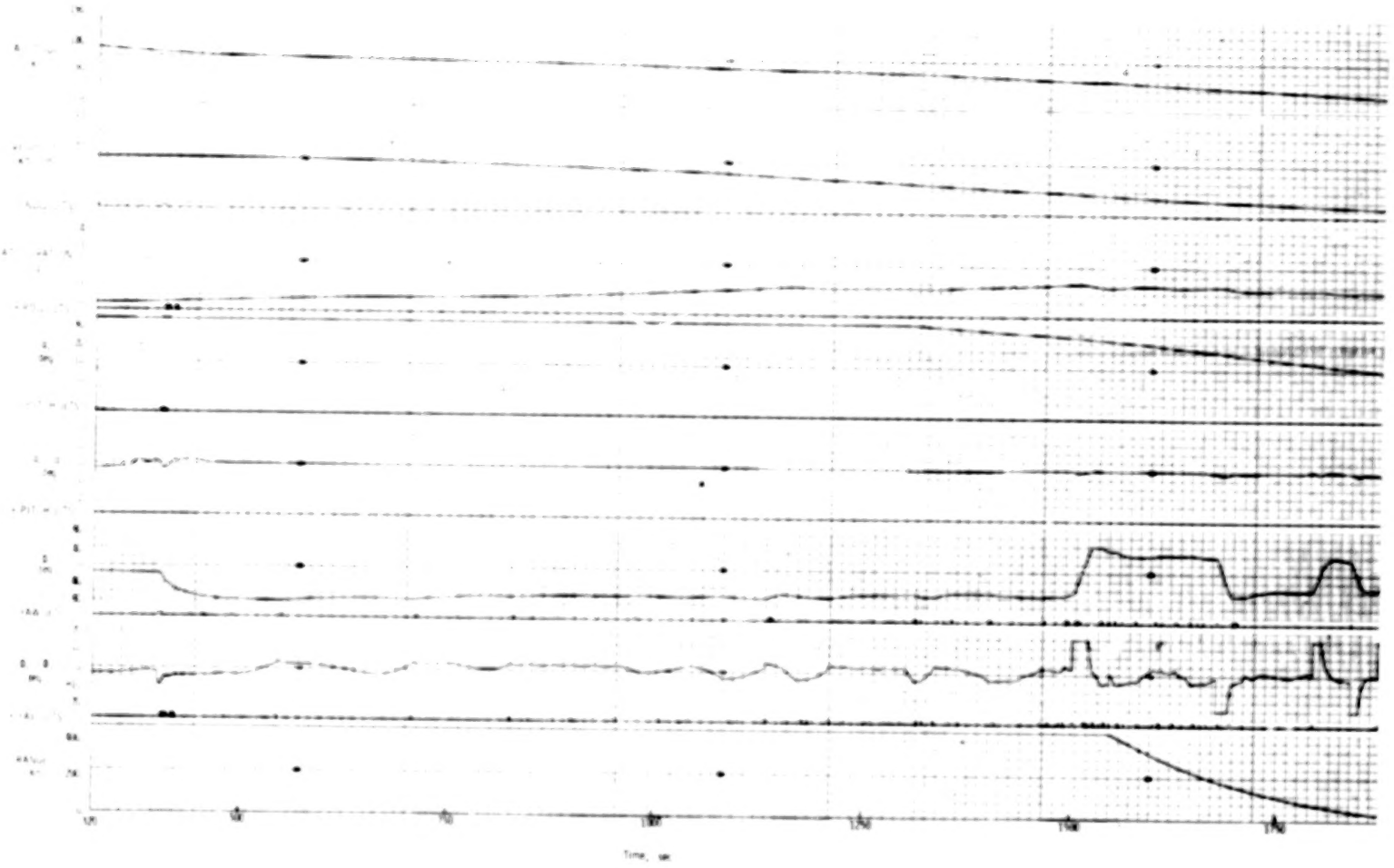

Figure 11.- Nominal guidance with hysteresis factors; $C_1 = 1.0$; $C_2 = -5^{\circ}$.

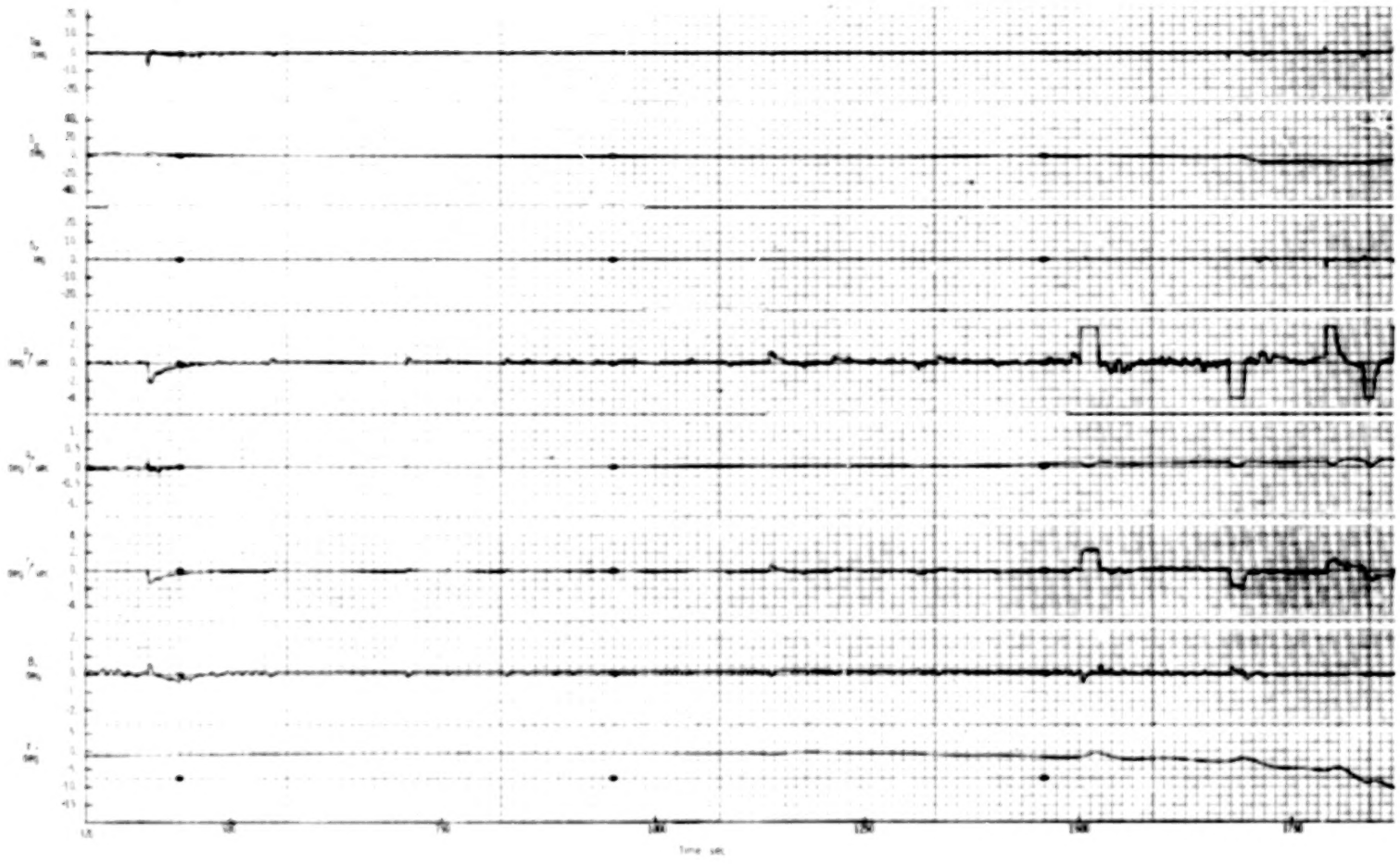

Figure 11.- Concluded.

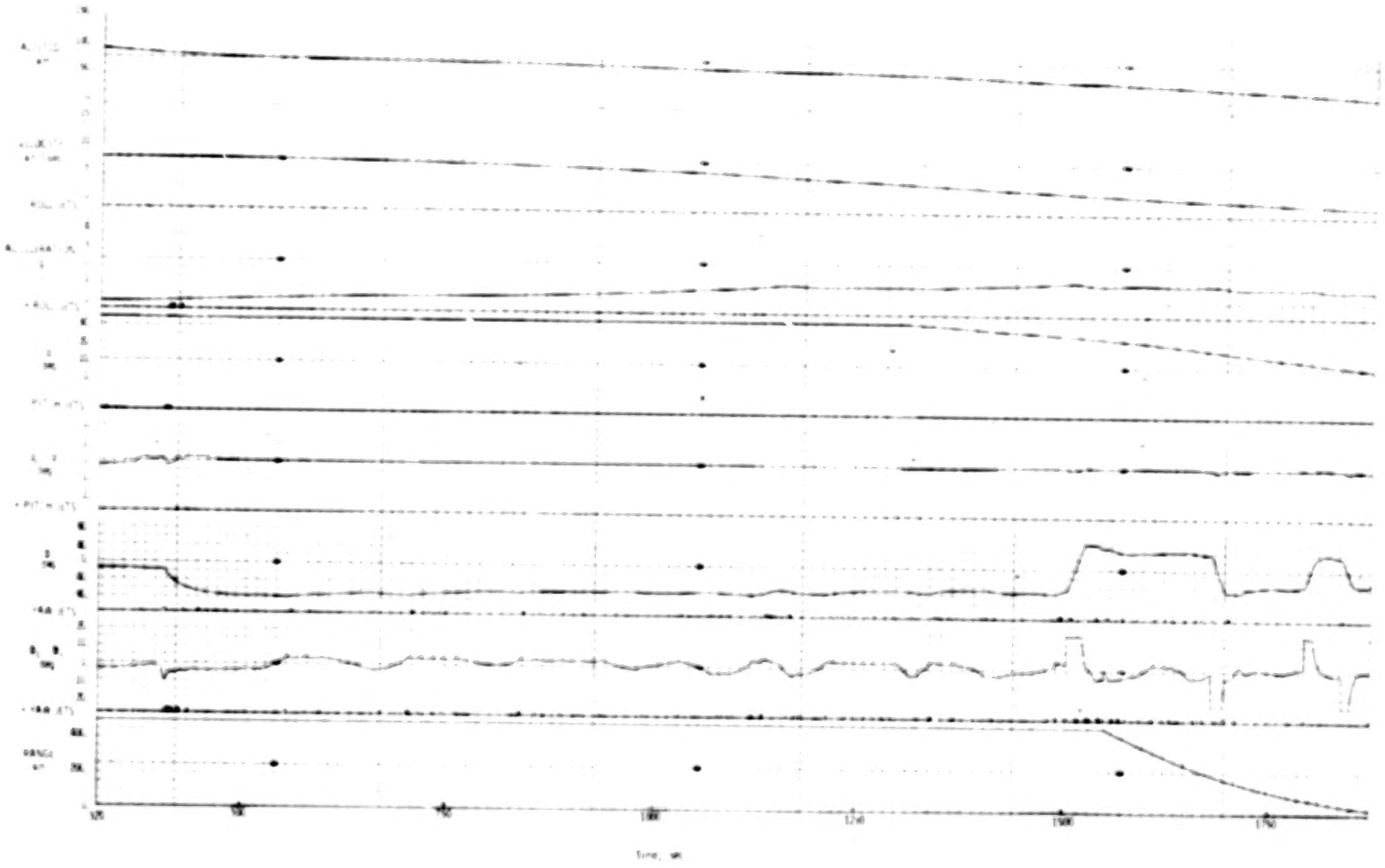

Figure 12.- Nominal guidance with hysteresis factors; $C_1 = 0.5$; $C_2 = -5^{\circ}$.

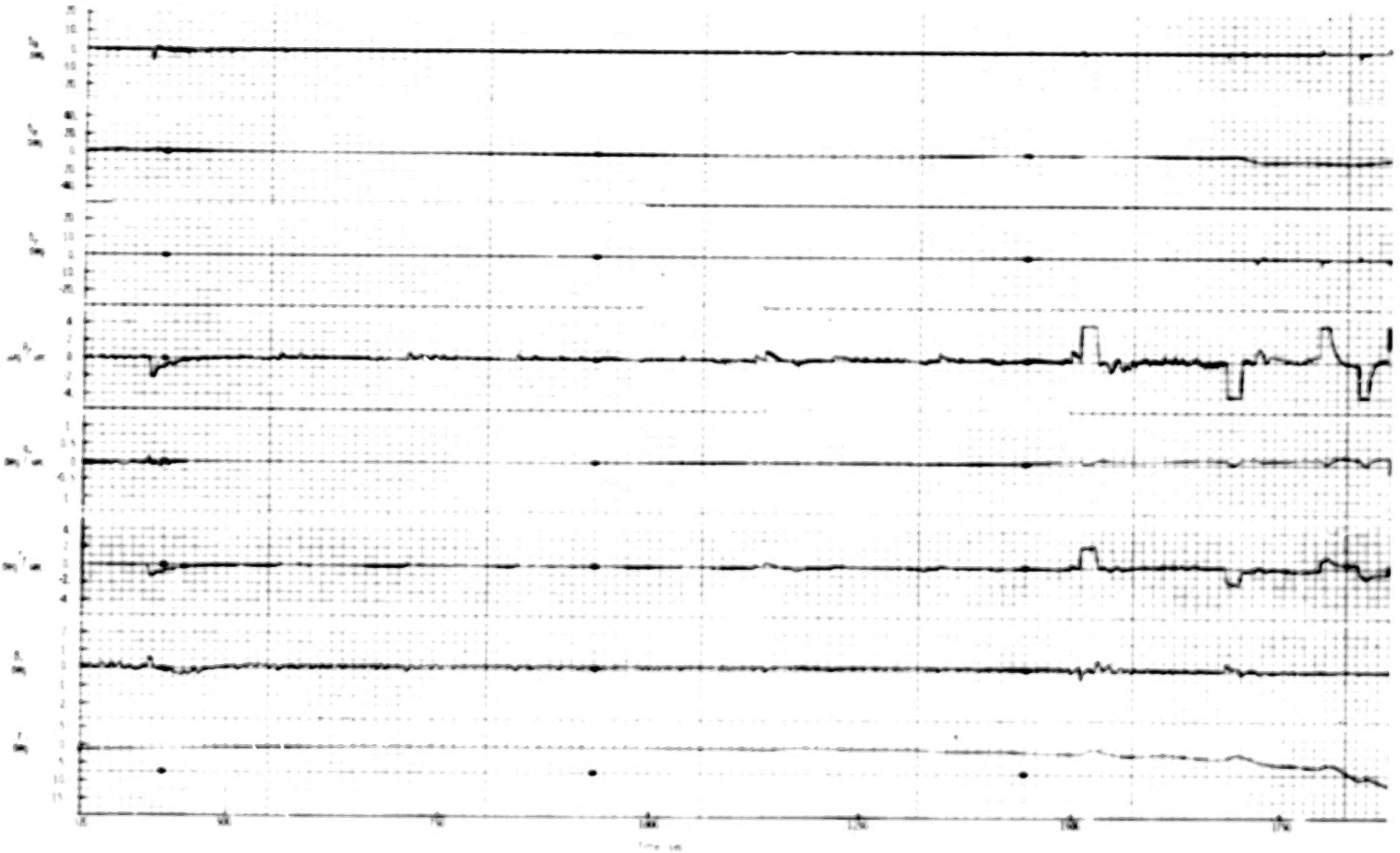

Figure 12.- Concluded.

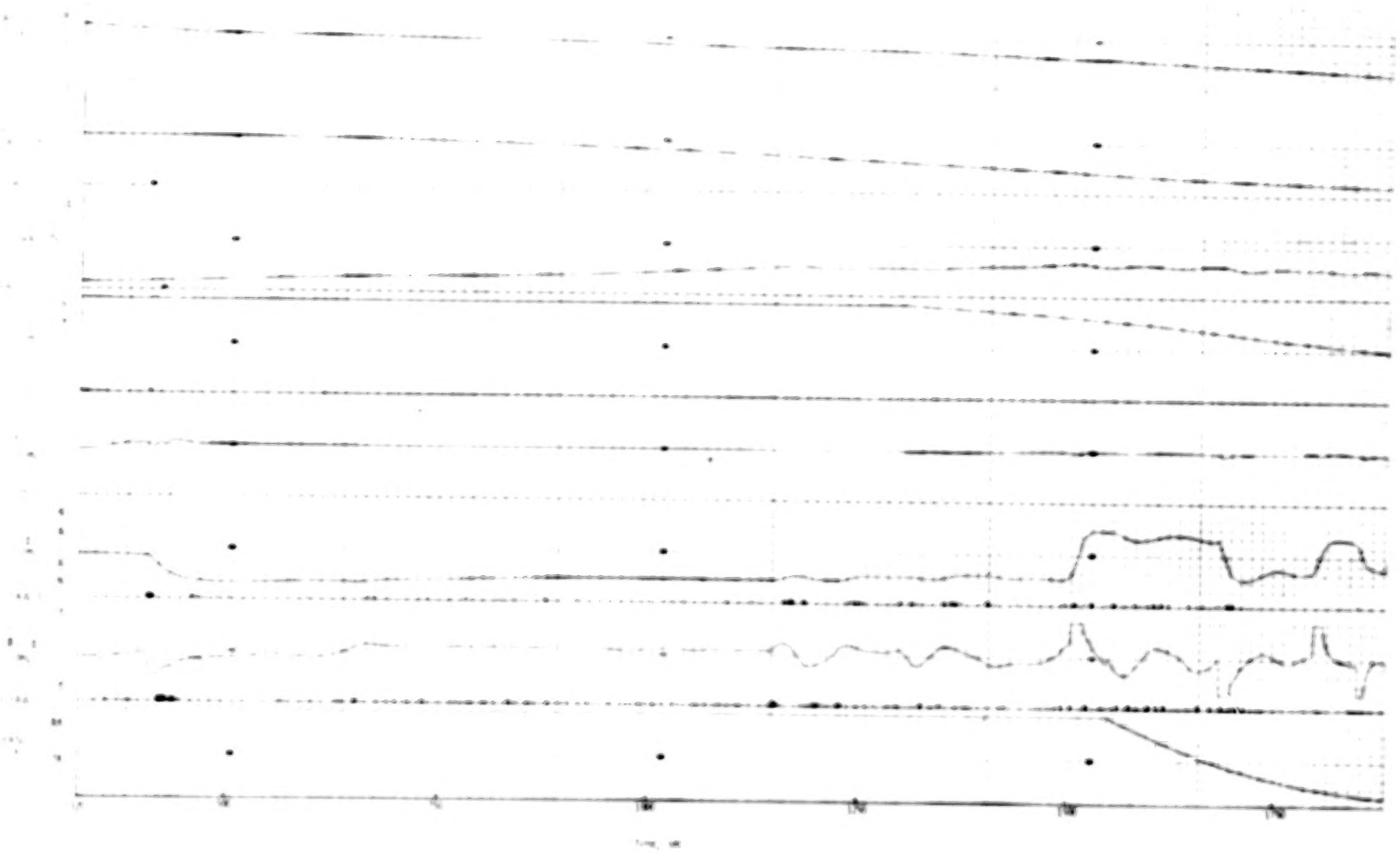

Figure 13.- Revised guidance with no hysteresis.

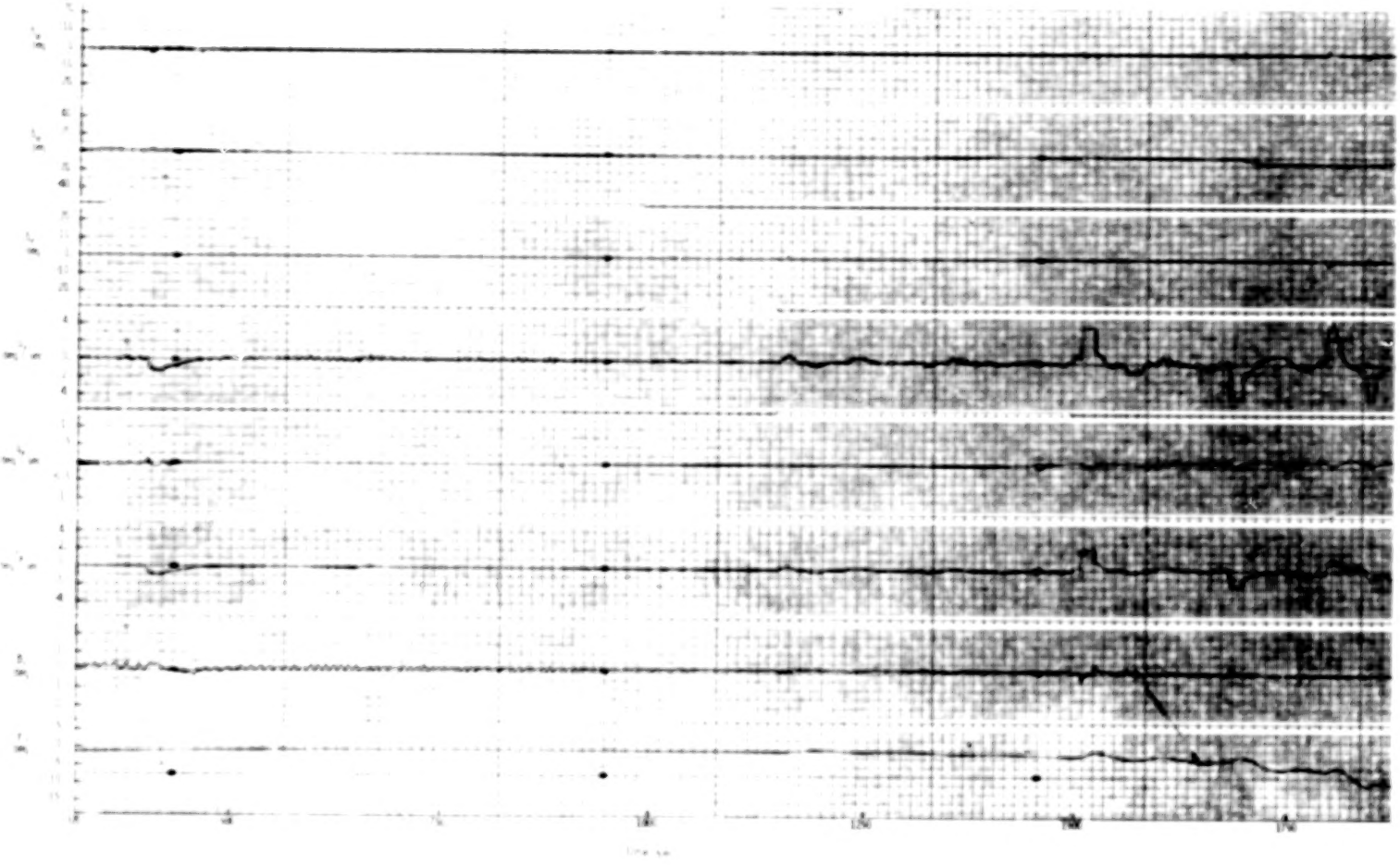

Figure 13.- Concluded.

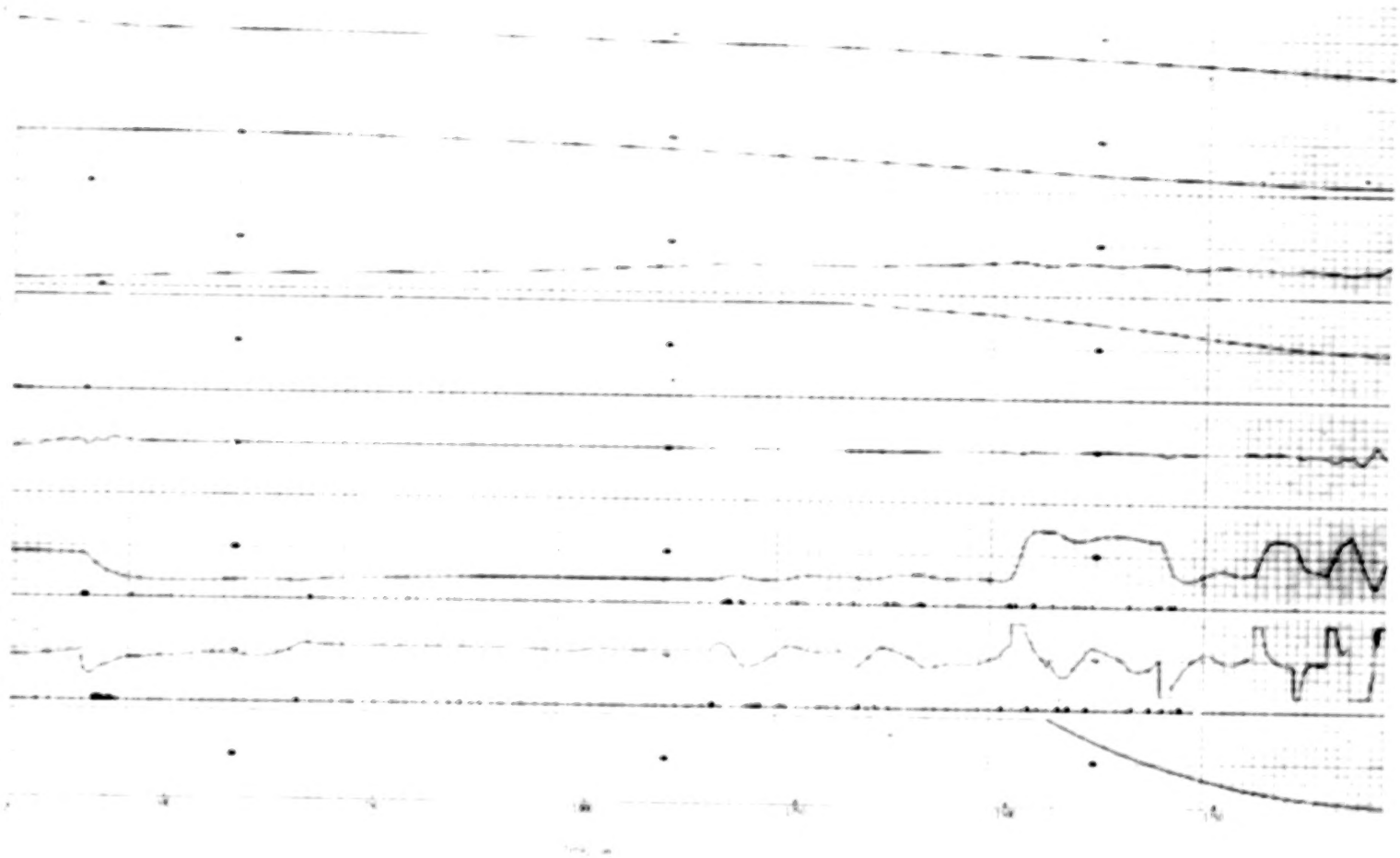

Figure 14.- Revised guidance with hysteresis factors; $C_1 = 0.7$; $C_2 = 0^{\circ}$.

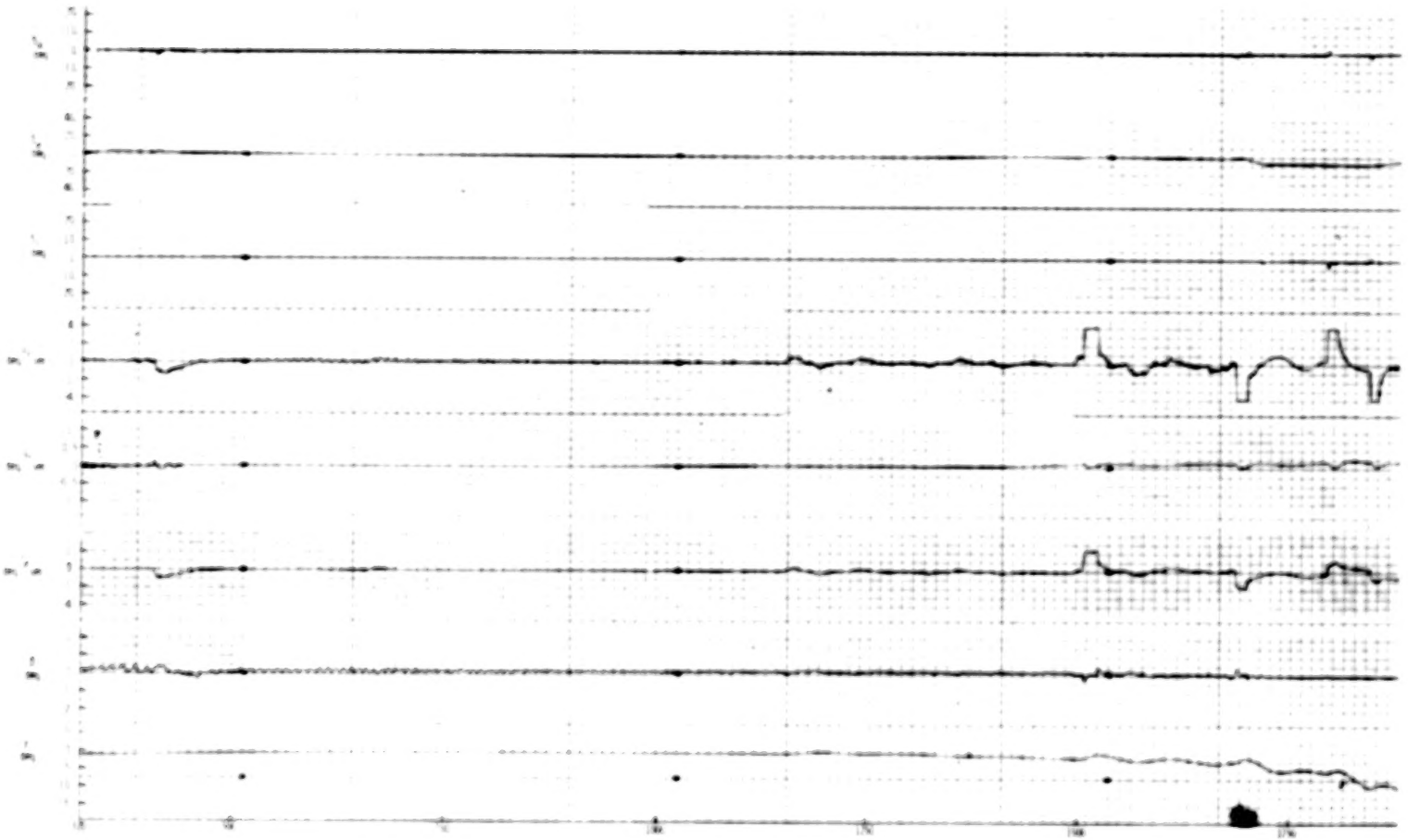

Figure 14.- Concluded.

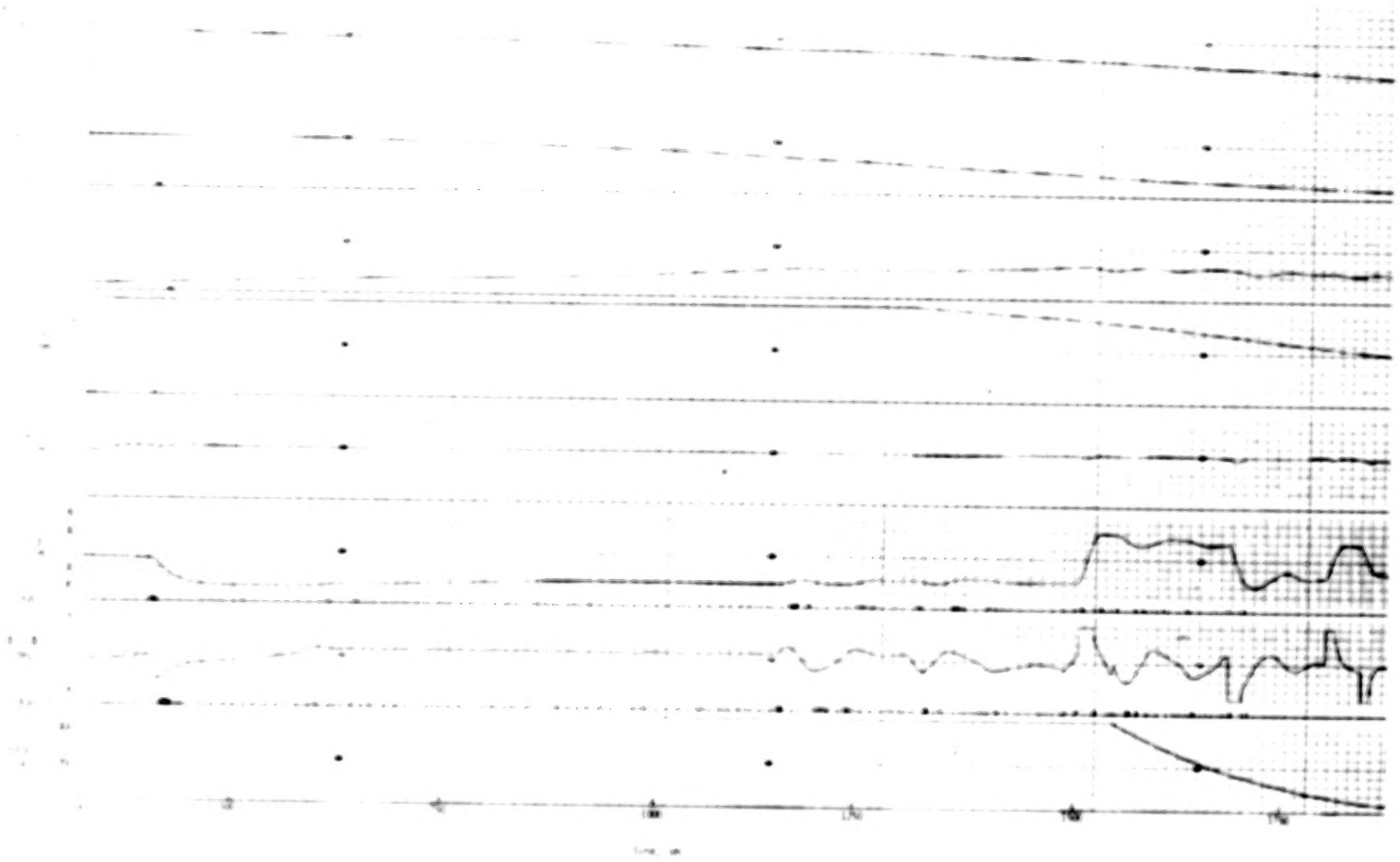

Figure 15.- Revised guidance with hysteresis factors; $C_1 = 0.5$; $C_2 = 0^\circ$.

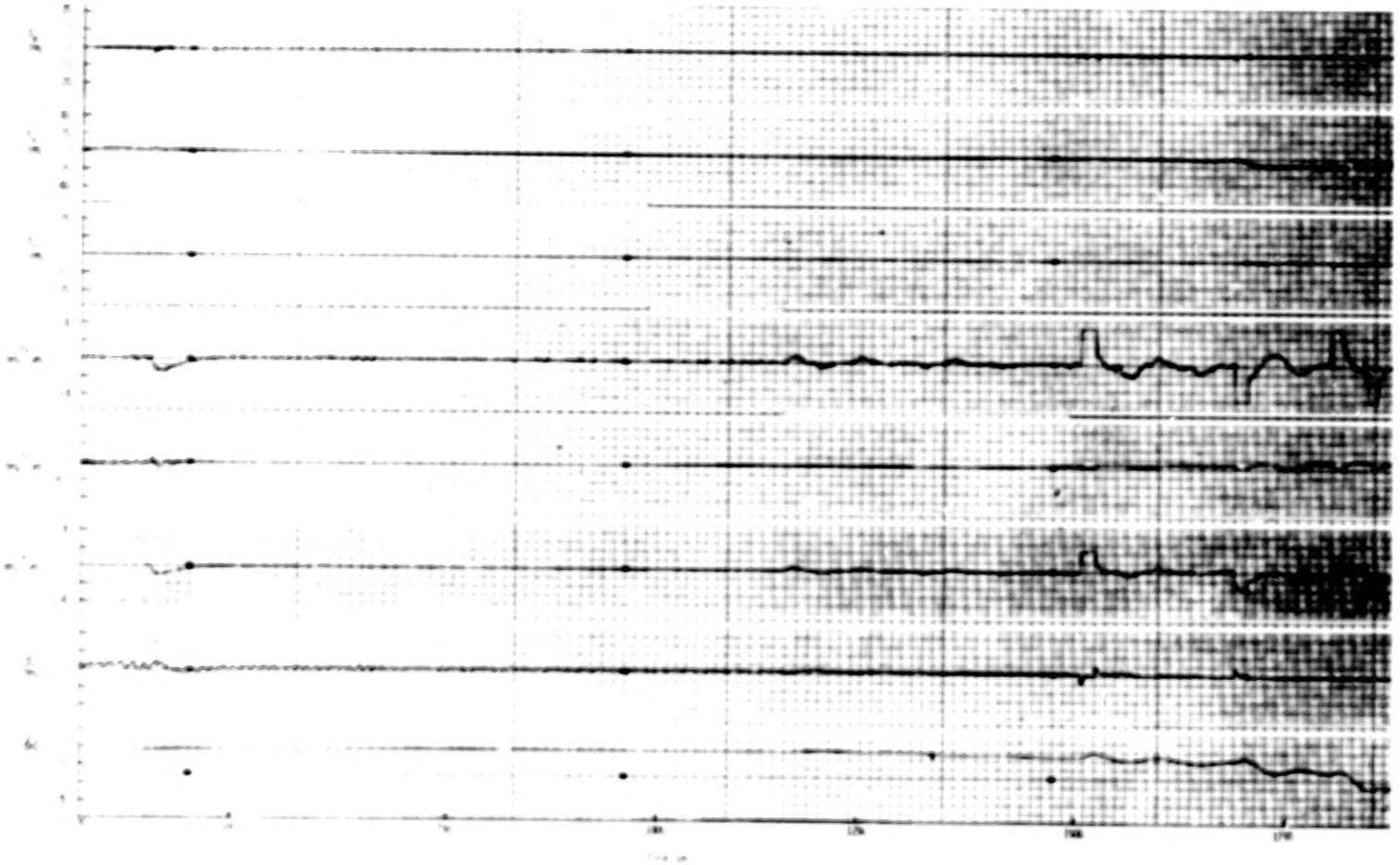

Figure 15.- Concluded.

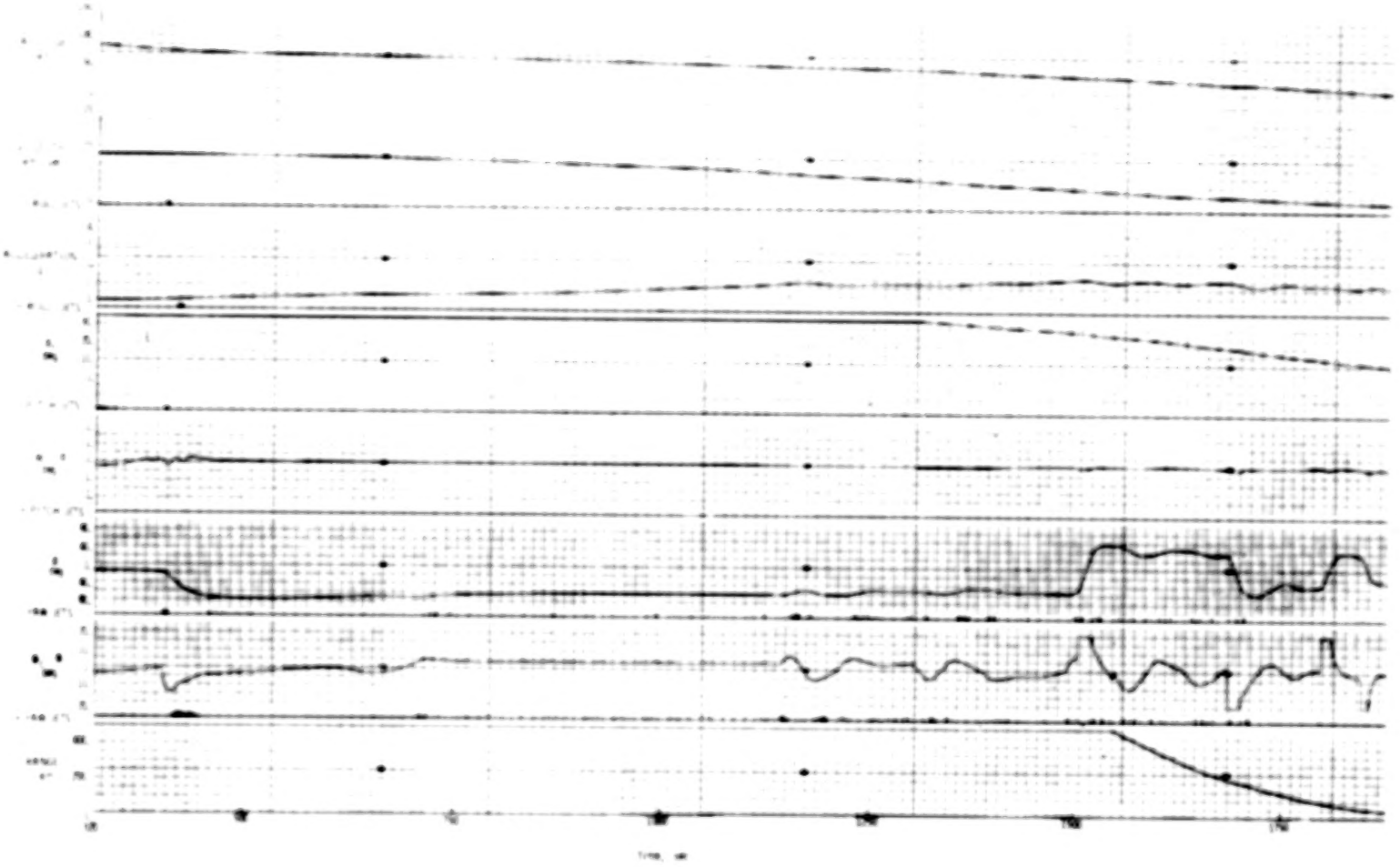

Figure 16.- Revised guidance with hysteresis factors; $C_1 = 1.0$; $C_2 = -2^{\circ}$.

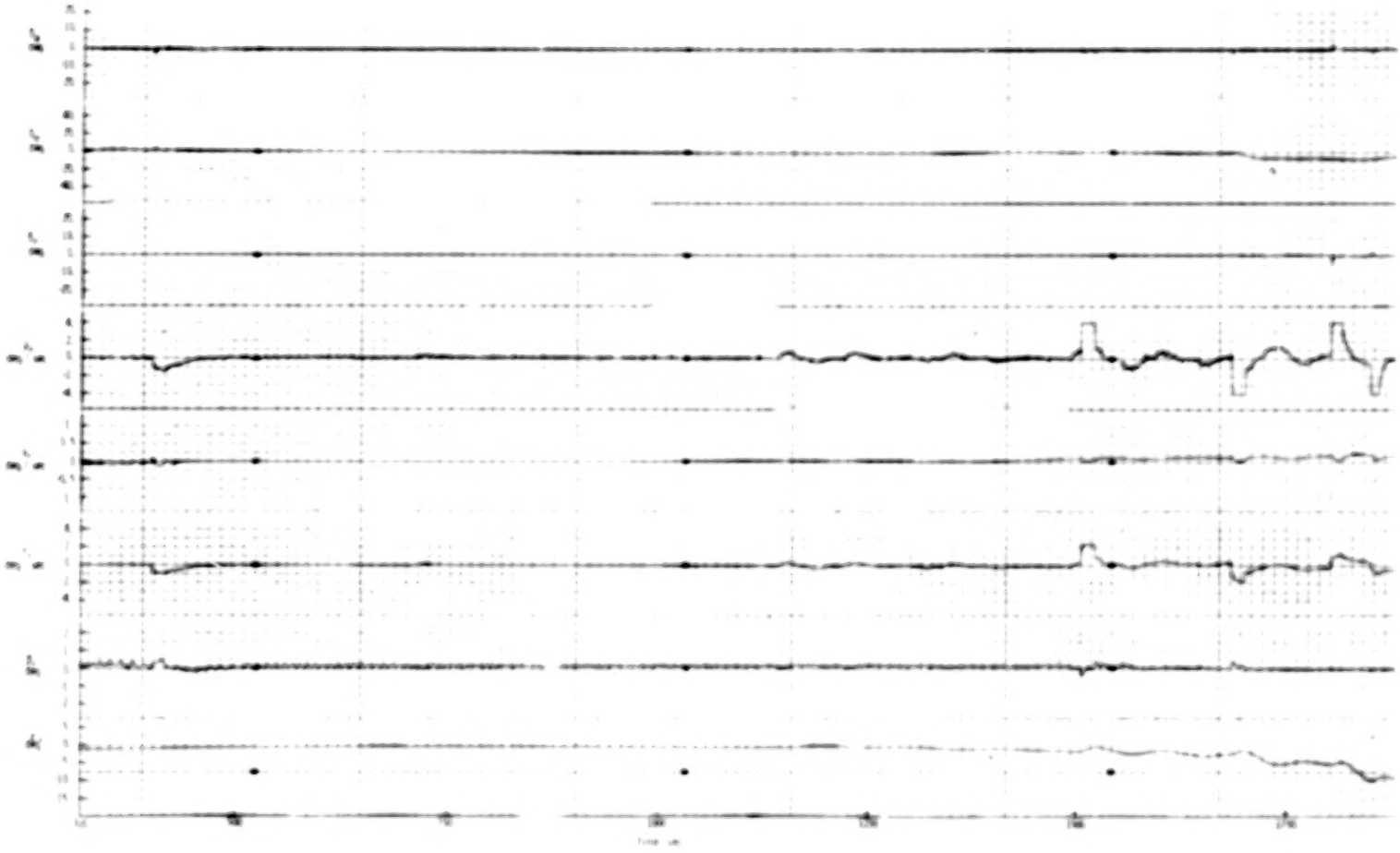

Figure 16.- Concluded.

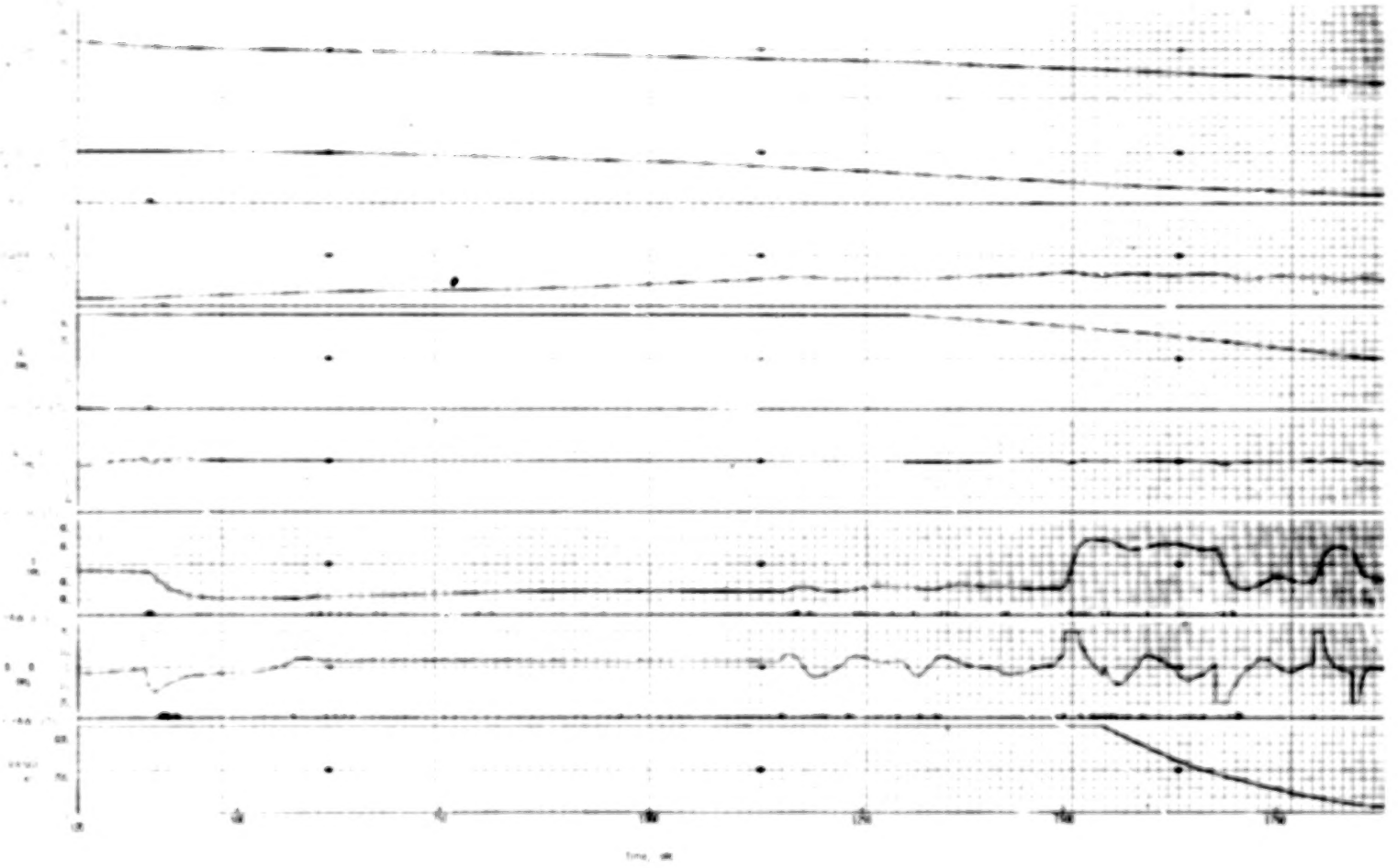

Figure 17.- Revised guidance with hysteresis factors; $C_1 = 1.0$; $C_2 = -5^\circ$.

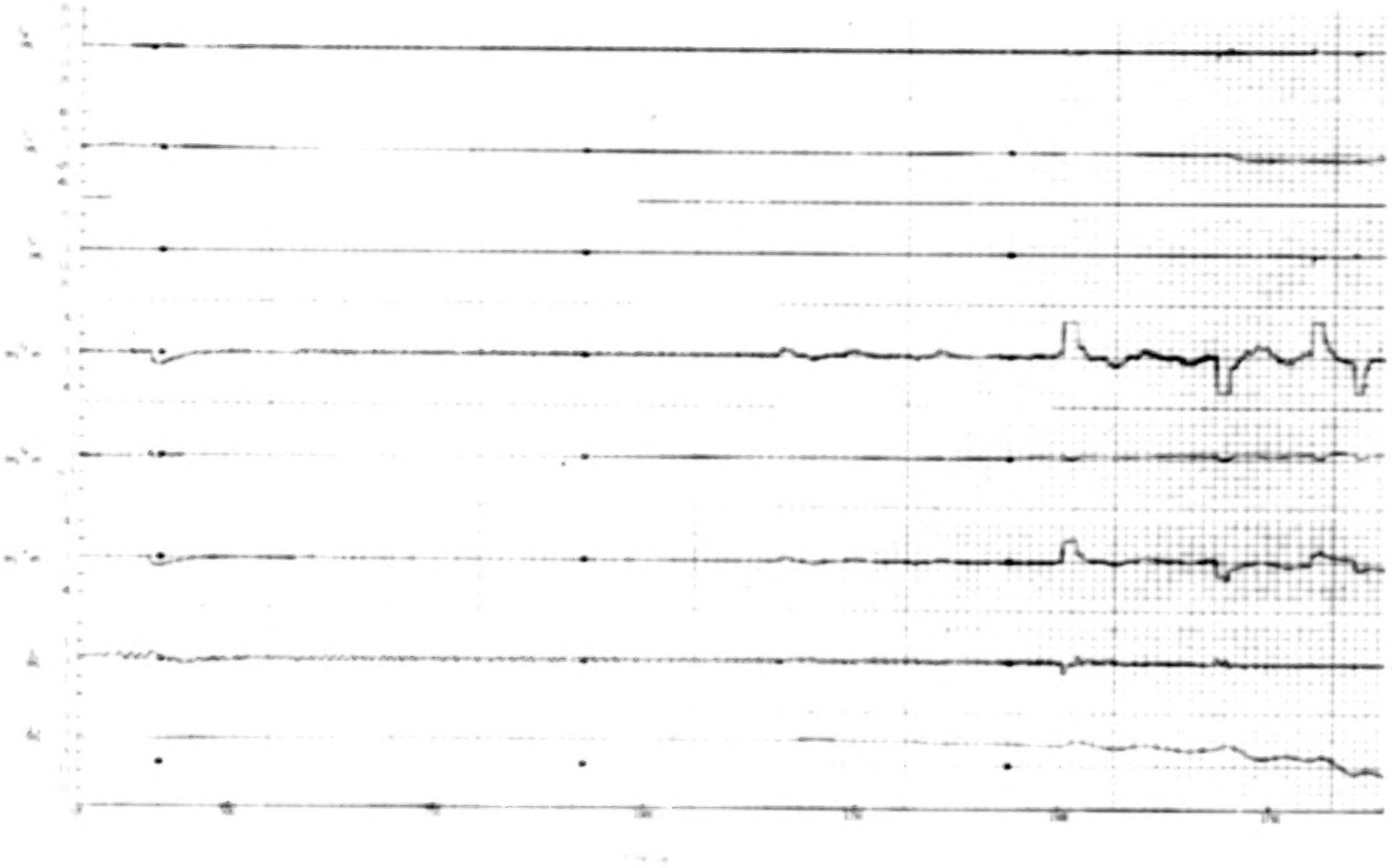

Figure 17.- Concluded.

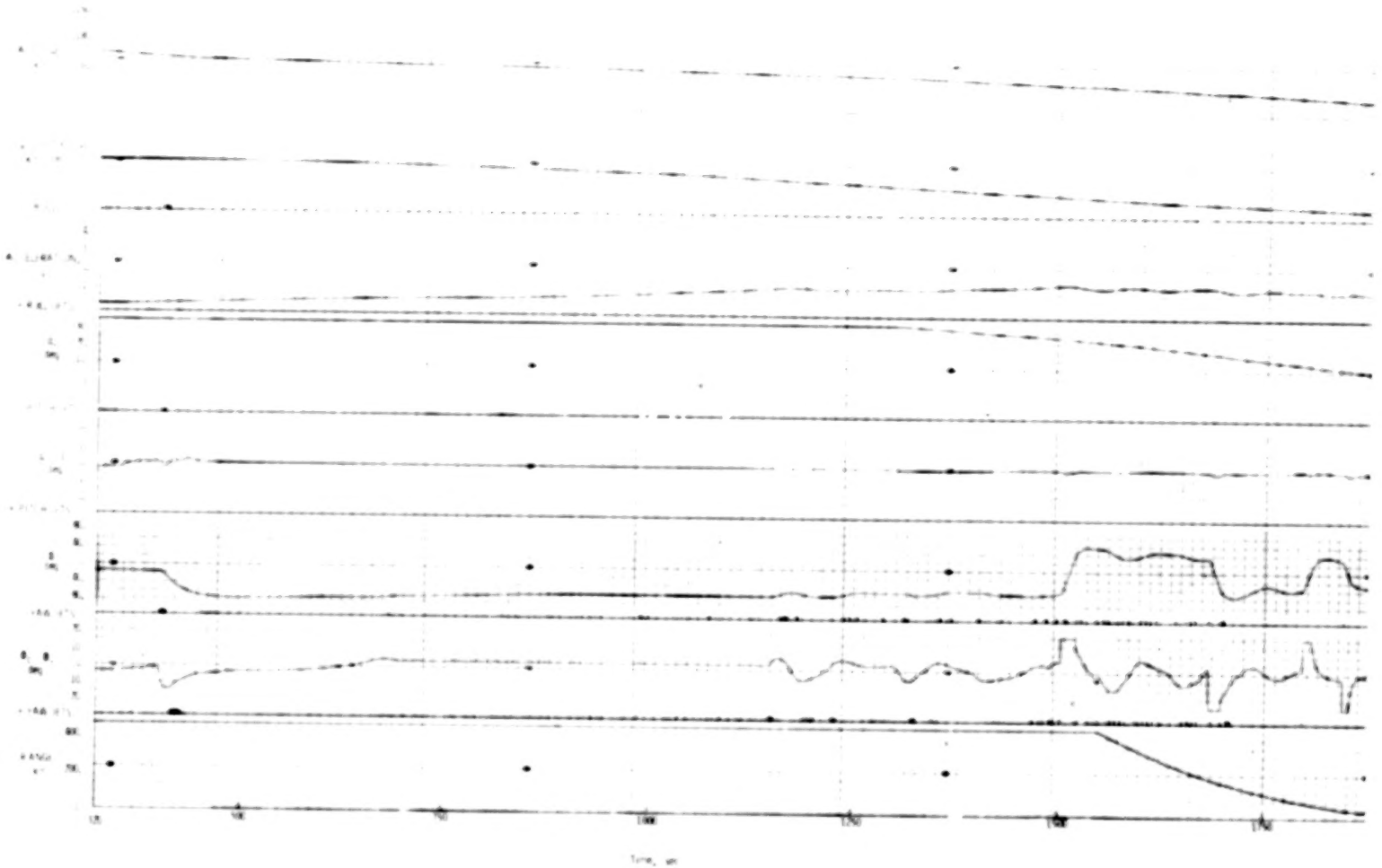

Figure 18.- Revised guidance with hysteresis factors; $C_1 = 0.5$; $C_2 = -5^{\circ}$.

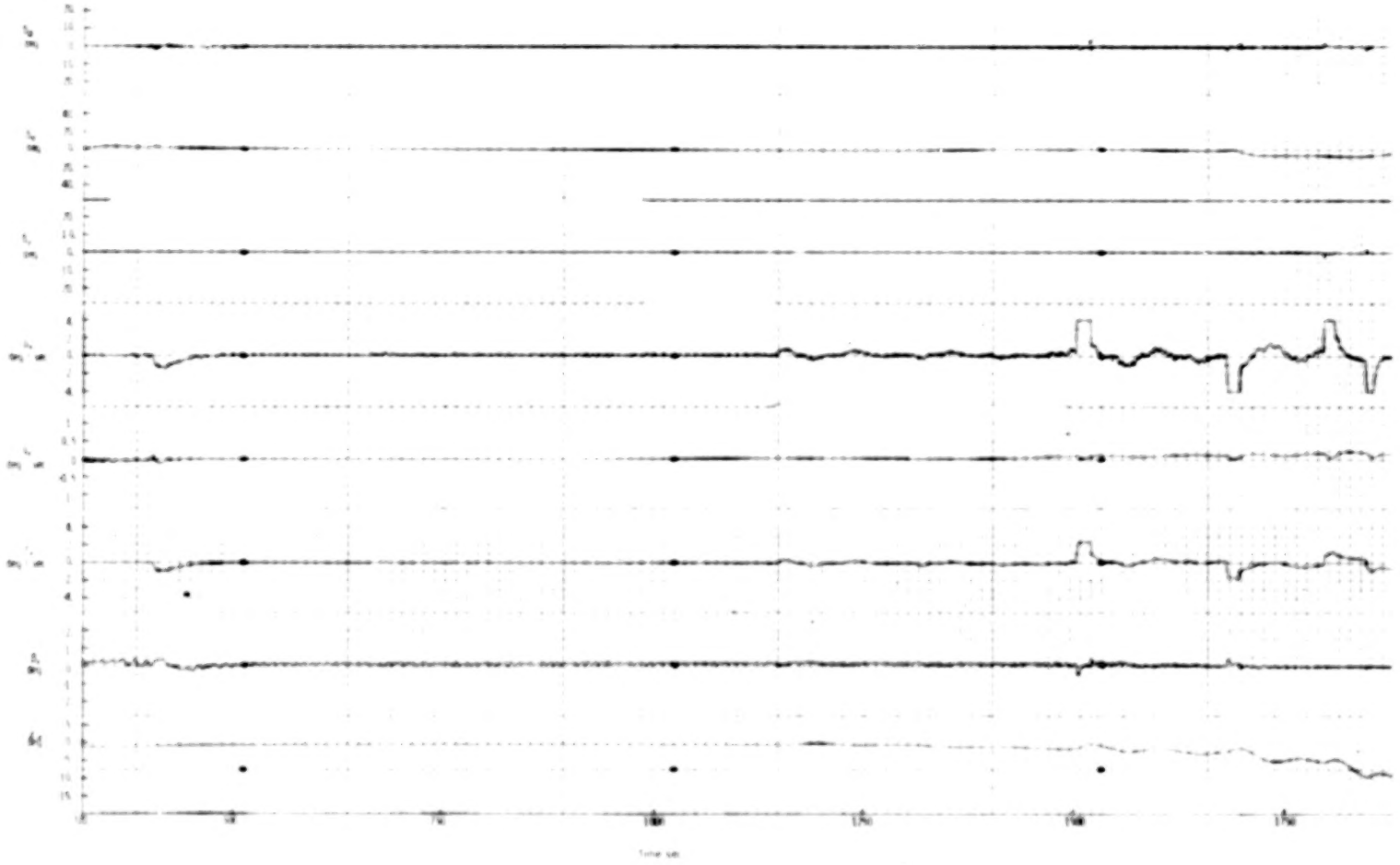

Figure 18.- Concluded.

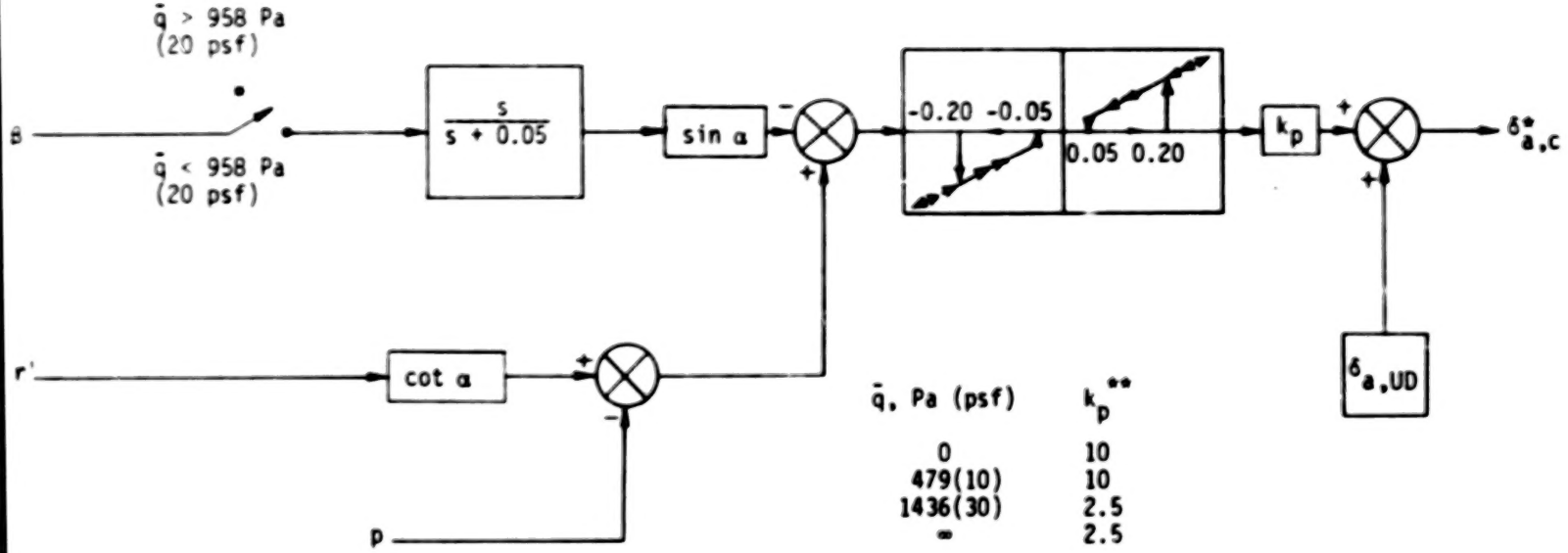

$\bar{q}$, Pa (psf)	k_p**
0	10
479(10)	10
1436(30)	2.5
∞	2.5

*For $\bar{q}$ < 92 Pa (2 psf), $\delta_{a,c}$ = 0.

**k_p linearly varied between indicated points.

Figure 19.- Aileron command block diagram for α > 18° or M > 5.

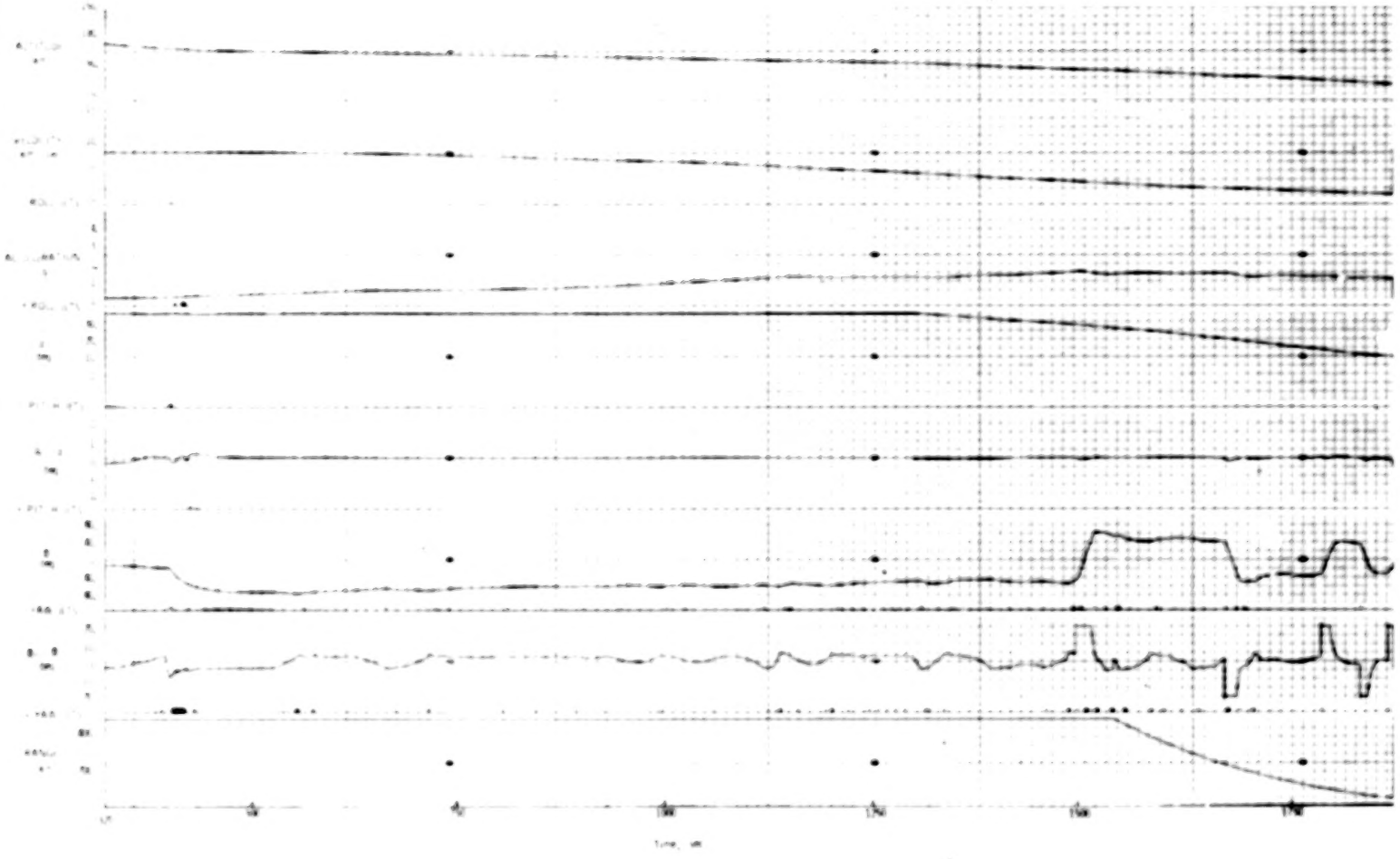

Figure 20.- Nominal guidance; no deadband in aileron control; no hysteresis.

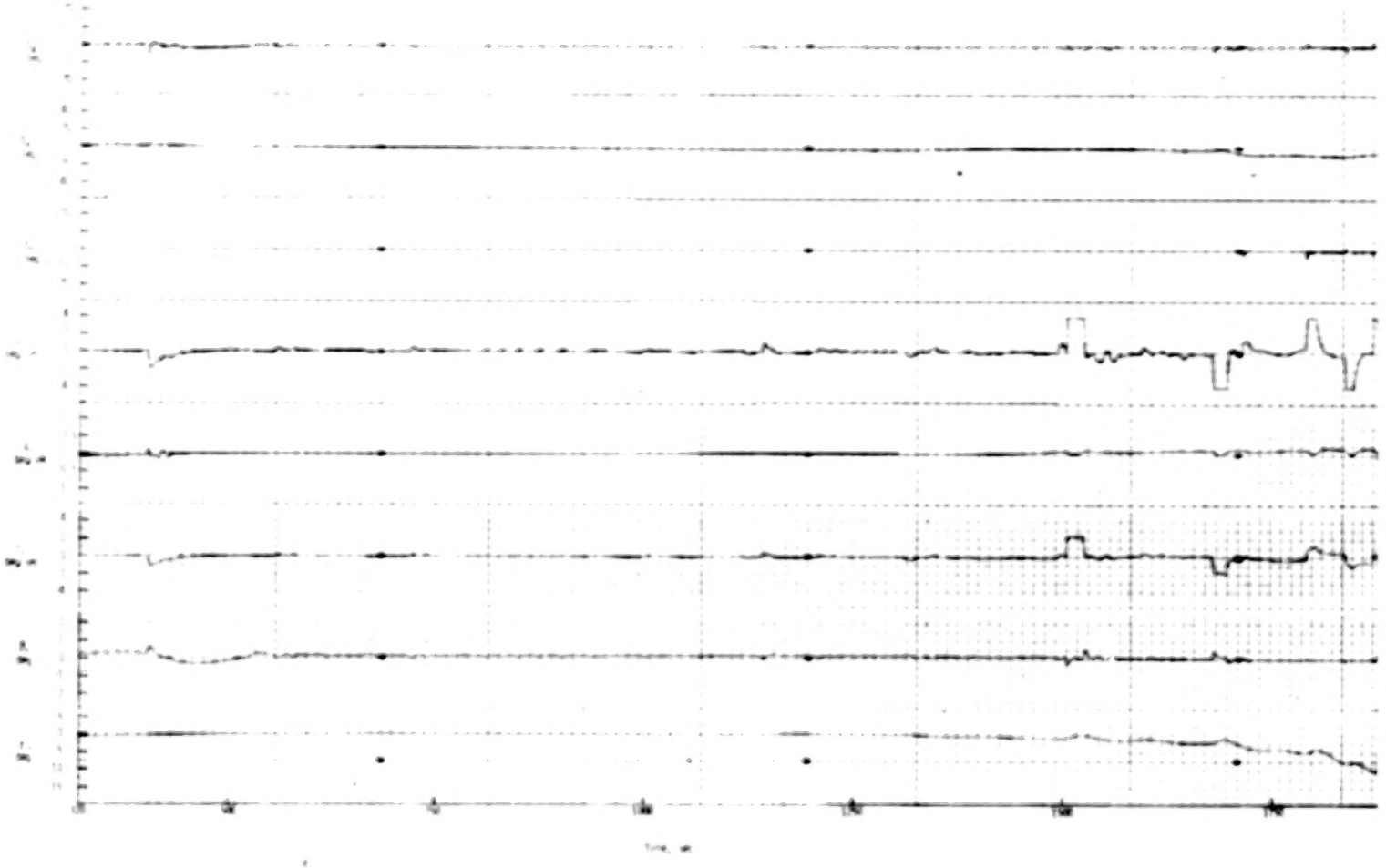

Figure 20.- Concluded.

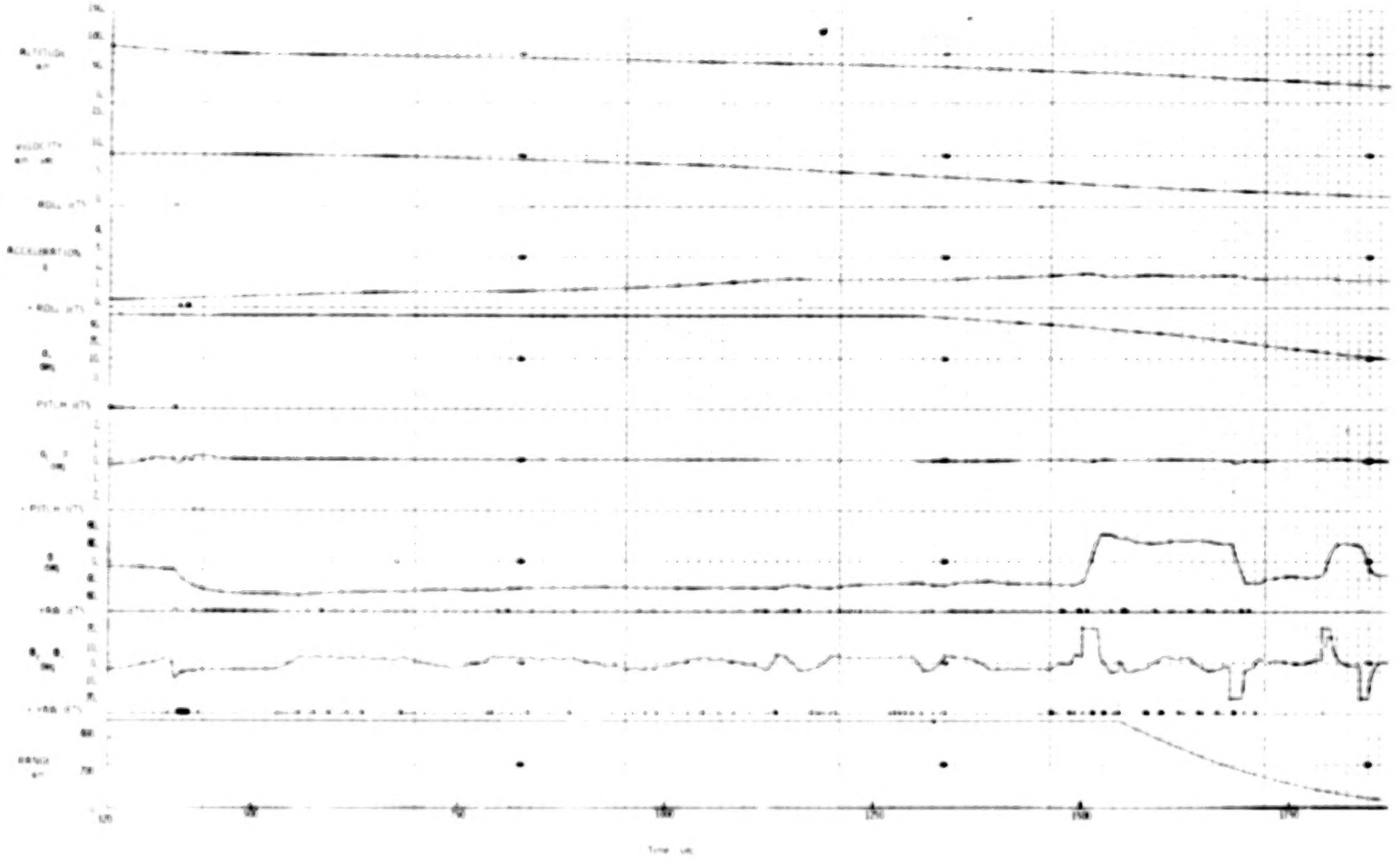

Figure 21.- Nominal guidance; no deadband in aileron control; hysteresis factors; $C_1 = 0.5$ and $C_2 = -5^{\circ}$.

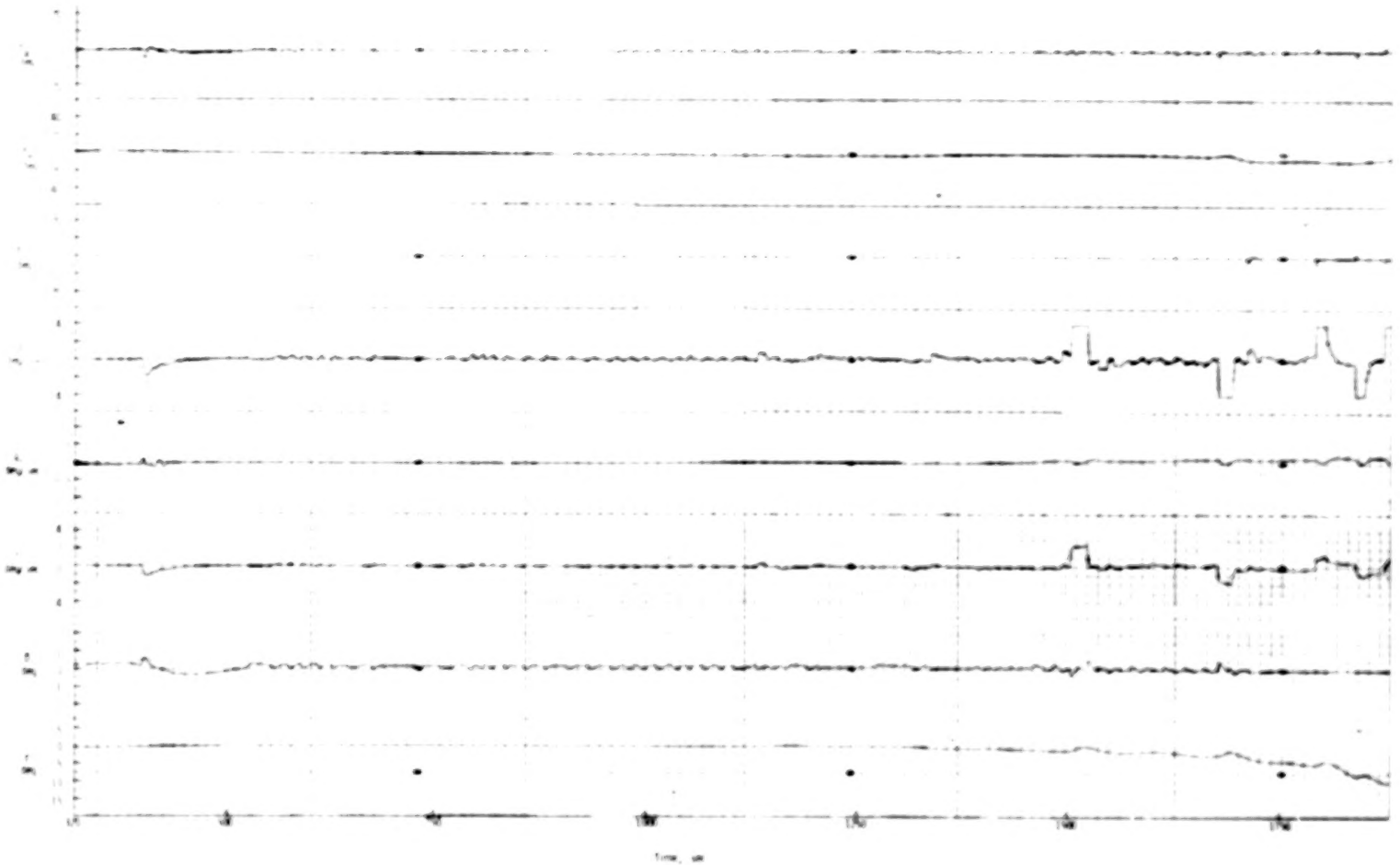

Figure 21.- Concluded.

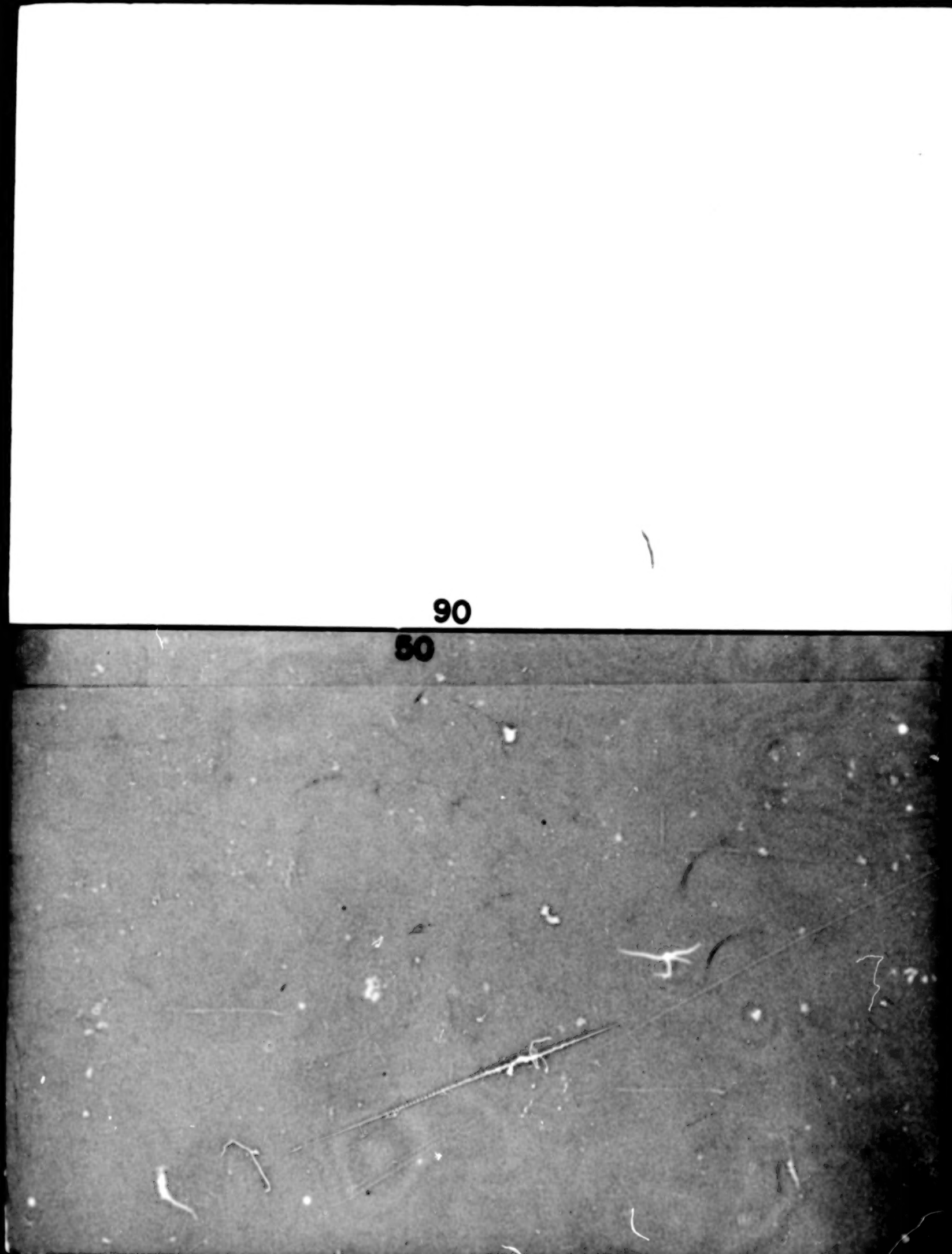
90
50

END

5.19 78